Journal of Environmental Management 270 (2020) 110905

Contents lists available at ScienceDirect

Journal of Environmental Management

journal homepage: http://www.elsevier.com/locate/jenvman

Research article

An agent-based model that simulates the spatio-temporal dynamics of sources and transfer mechanisms contributing faecal indicator organisms to streams. Part 2: Application to a small agricultural catchment

Aaron J. Neill [a,b,*], Doerthe Tetzlaff [c,d,a], Norval J.C. Strachan [e], Rupert L. Hough [b], Lisa M. Avery [b], Marco P. Maneta [f,g], Chris Soulsby [a,c]

[a] Northern Rivers Institute, University of Aberdeen, Aberdeen, AB24 3UF, Scotland, United Kingdom
[b] The James Hutton Institute, Craigiebuckler, Aberdeen, AB15 8QH, Scotland, United Kingdom
[c] IGB Leibniz Institute of Freshwater Ecology and Inland Fisheries, 12587, Berlin, Germany
[d] Department of Geography, Humboldt University Berlin, 10099, Berlin, Germany
[e] School of Biological Sciences, University of Aberdeen, Cruickshank Building, St Machar Drive, Aberdeen, AB24 3UU, Scotland, United Kingdom
[f] Geosciences Department, University of Montana, Missoula, MT, 59812-1296, USA
[g] Department of Ecosystem and Conservation Sciences, W.A Franke College of Forestry and Conservation, Universtiy of Montana, Missoula, USA

ARTICLE INFO

Keywords:
Diffuse pollution
E. coli
EcH_2O-iso
Microbial water quality
Tracer-aided modelling
Water quality modelling

ABSTRACT

The new Model for the Agent-based simulation of Faecal Indicator Organisms (MAFIO) is applied to a small (0.42 km^2) Scottish agricultural catchment to simulate the dynamics of *E. coli* arising from sheep and cattle farming, in order to provide a proof-of-concept. The hydrological environment for MAFIO was simulated by the "best" ensemble run of the tracer-aided ecohydrological model EcH_2O-iso, obtained through multi-criteria calibration to stream discharge (MAE: 1.37 L s^{-1}) and spatially-distributed stable isotope data (MAE: 1.14–3.02‰) for the period April–December 2017. MAFIO was then applied for the period June–August for which twice-weekly *E. coli* loads were quantified at up to three sites along the stream. Performance in simulating these data suggested the model has skill in capturing the transfer of faecal indicator organisms (FIOs) from livestock to streams via the processes of direct deposition, transport in overland flow and seepage from areas of degraded soil. Furthermore, its agent-based structure allowed source areas, transfer mechanisms and host animals contributing FIOs to the stream to be quantified. Such information is likely to have substantial value in the context of designing and spatially-targeting mitigation measures against impaired microbial water quality. This study also revealed, however, that avenues exist for improving process conceptualisation in MAFIO (e.g. to include FIO contributions from wildlife) and highlighted the need to quantitatively assess how uncertainty in the spatial extent of surface flow paths in the simulated hydrological environment may affect FIO simulations. Despite the consequent status of MAFIO as a research-level model, its encouraging performance in this proof-of-concept study suggests the model has significant potential for eventual incorporation into decision support frameworks.

1. Introduction

A prerequisite to improving impaired microbial water quality in agricultural catchments is identification of the sources and transfer mechanisms which contribute faecal indicator organisms (FIOs) to streams at the sub-field scale where mitigation measures can be implemented (Oliver et al., 2007, 2016; also c.f. Greene et al., 2015; Vinten et al., 2017). In a companion paper (Neill et al., 2020), limitations were identified in using existing process-based FIO models to understand sub-field-scale drivers of in-stream FIO dynamics that emerge at the catchment scale. Specifically, the coarse spatial discretisations often adopted by such models are inconsistent with the scales at which processes affecting FIO fate and transport operate and at which mitigation measures can be employed (Rode et al., 2010; Wellen et al., 2015). Furthermore, as most FIO models are aggregative (i.e. they simulate stores and fluxes of FIOs integrated over spatial units), the ability to

* Corresponding author. Northern Rivers Institute, University of Aberdeen, Aberdeen, AB24 3UF, Scotland, United Kingdom.
E-mail address: aaron.neill@abdn.ac.uk (A.J. Neill).

https://doi.org/10.1016/j.jenvman.2020.110905
Received 1 November 2019; Received in revised form 29 May 2020; Accepted 31 May 2020
Available online 13 July 2020
0301-4797/© 2020 Elsevier Ltd. All rights reserved.

account for heterogenity amongst FIOs of different types and to trace pathways taken by individual FIOs to streams is limited (c.f. O'Sullivan et al., 2012; Reaney, 2008). Finally, most FIO models rely on skill in simulating stream discharge to indicate whether catchment hydrological functioning is being adequately captured (Cho et al., 2016). However, such data do not contain information on the velocities of water through a catchment that reflect flow path dynamics and hydrological connectivity, factors to which FIO transport is sensitive (Birkel and Soulsby, 2015; Wellen et al., 2015).

Drawing on the potential offered by agent-based models for simulating individuals with heterogenous attributes that can be tracked over a simulation, Neill et al. (2020) reported the development of a new Model for the Agent-based simulation of Faecal Indicator Organisms (MAFIO) as an alternative approach to FIO modelling. The purpose of the model is to elucidate the sources and transfer mechanisms contributing FIOs to streams at the sub-field scale in small (<10 km^2) agricultural catchments through simulating and tracking the fate and transport of agents representing FIOs (FIO-agents) in a process-based, spatially--distributed manner. MAFIO consists of six sub-models that allow simulation of the following processes: 1) FIO loading from different livestock, including direct deposition in streams; 2) FIO die-off as a function of temperature and, for above-ground FIOs, solar radiation; 3) Detachment of FIOs from faeces; 4) Surface routing of FIOs accounting for infiltration, exfiltration and lateral transport in overland flow; 5) Seepage of FIOs to streams from areas of degraded soil; 6) Channel routing with settling modelled by a distance-decay function for sediment-associated FIOs. A further key feature of MAFIO is that the hydrological environment used to simulate hydrological transfer mechanisms is provided by an external model; thus, there is scope for using hydrological models which can be robustly evaluated with respect to their consistency with internal catchment states and process representation. Full details of the model, its operation and parameterisation can be found in the companion paper (Neill et al., 2020).

Here, MAFIO is applied to simulate the dynamics of *E. coli* in a small agricultural catchment in Scotland arising from sheep and cattle farming, in order to provide a proof-of-concept. The following specific questions are addressed:

1. To what extent can MAFIO resolve the main processes driving observed dynamics of FIOs?
2. What potential does MAFIO have for providing processed-based insights into microbial water quality that are relevant for management?

Given the potential of tracer-aided ecohydrological models in providing robust simulations of catchment hydrological functioning (see Neill et al., 2020), the model EcH$_2$O-iso (Kuppel et al., 2018a) is used to generate the hydrological environment for MAFIO following multi-criteria calibration to discharge and spatially-distributed isotope data.

2. Study site

The study site was the Tulloch Burn catchment (0.42 km^2; Fig. 1a), a sub-catchment of the Tarland Burn (71 km^2) which is a tributary of the River Dee, NE Scotland. The Dee is a regional water resource, supplying >300,000 people with drinking water, and is designated a Special Area of Conservation due to the freshwater ecosystem it supports. Higher intensities of agriculture in lowland tributaries of the Dee have been linked to impaired water quality (Langan et al., 1997). As the most upstream tributary draining significant areas of agriculture, the Tarland Burn catchment became a research site for assessing diffuse- and point-sources of pollution and evaluating best management practices for mitigation (Bergfur et al., 2012). The selection of the Tulloch Burn catchment for this study was based on work that identified it as a "hot spot" for faecal contamination from 11 years of *E. coli* data (Neill et al., 2018).

Longer-term data (2000–2010) from Aboyne meteorological station ~10 km from the Tulloch shows mean annual precipitation and potential evapotranspiration for the area to be 828 mm and 521 mm, respectively (Dunn et al., 2013). Catchment elevation ranges from 216 m to 453 m. Brown earths (41%) and humus-iron podzols (34%) are the predominant soil-types (Fig. 1b; Soil Survey of Scotland Staff, 2014). These are freely-draining soils; consequently, artificial field drainage is not necessary in the catchment. There are also limited areas of non-calcareous gleys and alluvial soils, with higher elevations dominated by peaty-gleyed podzols (Fig. 1b; Soil Survey of Scotland Staff, 2014). Approximately 60% of the catchment is agricultural (Fig. 1c). During the study, surveys showed that five fields were used for pastoral (sheep and cattle) farming (Lower/Mid Pasture [L/R] and Top Pasture) and two for arable (Lower/Upper Arable). Apart from Mid-Pasture (R), field boundaries extend beyond the Tulloch Burn catchment. Of the remaining catchment, 24% is mixed-conifer forest and 16% is heather moorland (Fig. 1c).

To prevent livestock access, parts of the stream are fenced-off from fields and surrounded by small riparian areas (Fig. 1d). However, stretches of the stream running through Mid Pastures (R) and (L) are directly accessible to livestock, with animals able to move between Mid Pastures (R) and (L) at a discrete stream crossing-point depending on whether a gate is open (Fig. 1c and e). Other discrete crossing-points can also connect Lower Pastures (R) and (L), and Lower Pasture (L) and Mid Pasture (R), again depending on gates (Fig. 1c). Observation during the study found a high degree of soil compaction around all three crossing points (DS1-3 in Fig. 1c) due to the concentration of livestock moving through these areas. This resulted in the soils being in a state of semi-permanent saturation (Fig. 1f); therefore, these areas of degraded soil can continually seep water to the stream and may be a potential source of chronic faecal contamination (e.g. Bilotta et al., 2007).

3. Data and methods

3.1. Hydrometric and isotope data

Hydrometric monitoring at the Tulloch Burn started in October 2016. The main study period was between 27/04/17 and 31/12/17. Daily average discharge at the catchment outlet and sites T6 and T8 was derived by area-scaling discharge measurements made at the outlet of the 3.9 km^2 Blackmill Burn catchment within which the Tulloch is nested. Specifically, near-concurrent discharge (Q) measurements made under identical hydroclimatic conditions at five sites within the Blackmill Burn (including the outlet of the Tulloch) with catchment areas (A) of 0.2–3.9 km^2 revealed a strong relationship between discharge and area ($Q = 1.85e\text{-}8 \times A^{0.97}$; Adj. R^2: 0.99). Consequently, discharges for sites within Tulloch Burn could be derived as:

$$Q_{TulX} = Q_{BM} \cdot \left(\frac{A_{TulX}}{A_{BM}}\right)^{0.97} \quad (1)$$

where Q_{TulX} and A_{TulX} are discharge and catchment area for Site X in the Tulloch Burn, respectively, and Q_{BM} and A_{BM} are discharge and catchment area of the Blackmill Burn, respectively. This was necessary as the narrow, poorly-defined channel of the Tulloch prevented a reliable stage-discharge rating curve. The Blackmill and Tulloch Burns have comparable soils and land use causing them to exhibit similar hydrological responses. Meteorological data (precipitation, temperature, relative humidity and windspeed) were collected at 15-mintue intervals using an automatic weather station within the catchment (Fig. 1a). Short- and long-wave radiation were obtained from ERA-Interim climate reanalysis (Dee et al., 2011). These data were amalgamated into daily timeseries.

Isotope samples were analysed for δ^2H and $\delta^{18}O$ using a Los Gatos laser isotope analyser (precision: ± 0.4‰ for δ^2H and 0.1‰ for $\delta^{18}O$).

Given higher relative precision, δ^2H was used here. Daily streamwater samples at the catchment outlet were collected for isotope analysis using an ISCO-3700 autosampler from 27/04/17 (Fig. 1a). A layer of paraffin was added to bottles to prevent evaporation. Synoptic grab-sampling for isotopes occurred on a twice-monthly basis at sites T2-8 (Fig. 1a). During the microbial observation period (Section 3.2), samples were taken twice-weekly at T6 and T8 to be coincident with samples taken for *E. coli* analysis. Daily bulk samples of precipitation were also collected using an ISCO-3700 autosampler.

3.2. Microbial and livestock count data

Within the study, a more intense field campaign was carried out between 08/06/17 and 31/08/17 (the "microbial observation period" – MOP) to collect higher-temporal-resolution data for stream *E. coli* concentrations and livestock counts. This corresponded to when most livestock are in the fields and potential for faecal contamination is elevated (Kay et al., 2008). Twice-weekly sampling for *E. coli* occurred during this period at the outlet, and from 06/07/17 at T6 and T8 to

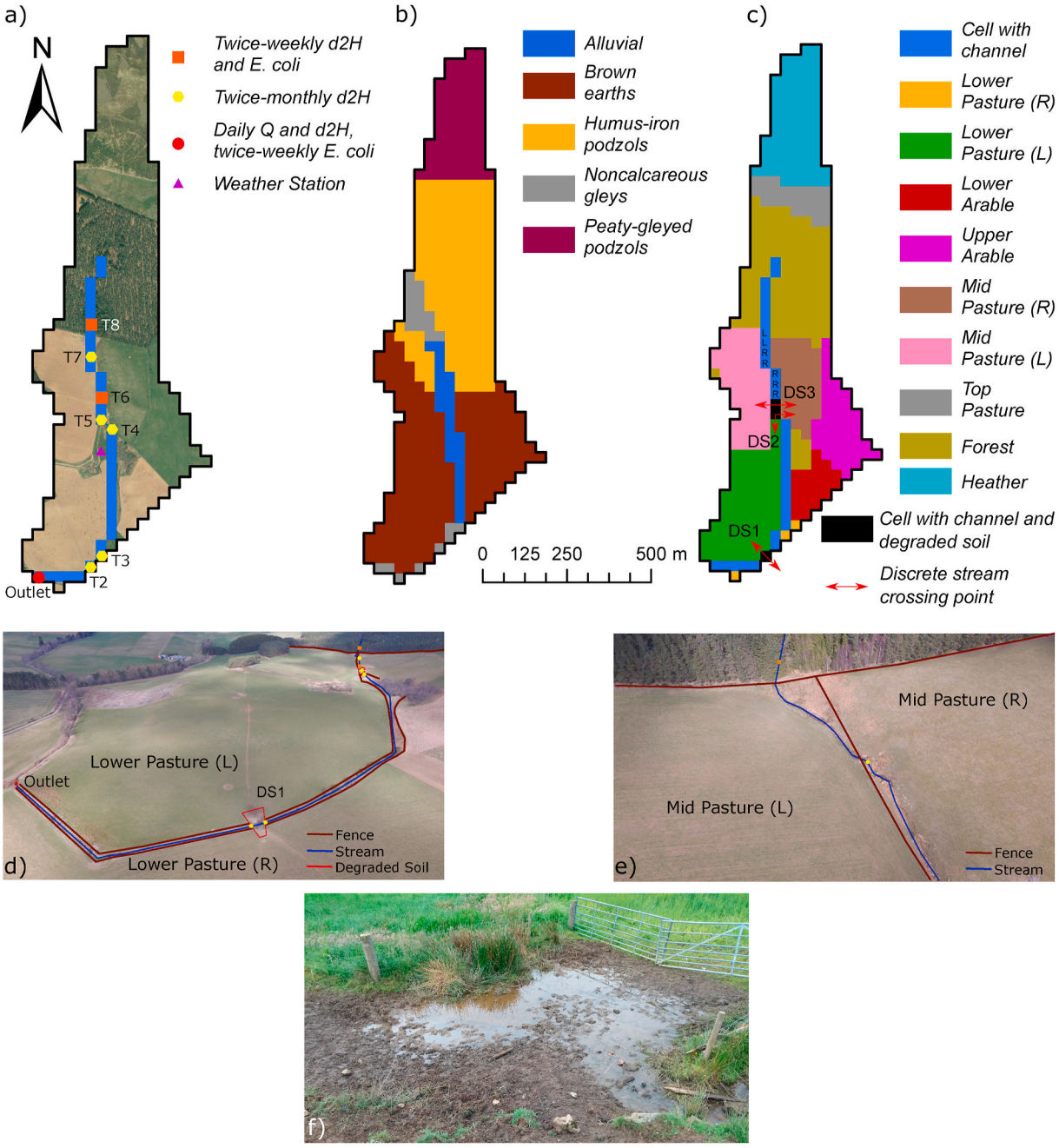

Fig. 1. The Tulloch Burn catchment, with maps showing a) An overview of the catchment and monitoring locations; b) Soil types based on Soil Survey of Scotland Staff (2014); c) Designations of land parcels and cells containing a channel (potentially with an area of degraded soil) as provided to MAFIO. In the latter, the appearance of "L" or "R" in cells containing a channel denote the permanent direct accessibility of the stream to livestock in Mid Pastures (L) and (R), respectively, whilst DS1-3 are the designations given to the three areas of degraded soil associated with discrete stream crossing points. The stream in (a) and all data in (b) and (c) are presented on the 30 × 30 m grid utilised by EcH$_2$O-iso and MAFIO. Also provided are drone-based aerial images of the catchment showing examples of d) Fencing-off of the stream from adjacent fields and areas of soil degradation; e) Sections of the stream directly accessible to livestock. For context, selected land parcel and degraded soil designations and approximate sampling locations are provided in the aerial images using the same symbols as in a). An example of soil degradation (DS3) in the catchment is shown in (f).

characterise spatial variability in concentrations arising from differing catchment characteristics (Fig. 1a). Samples for *E. coli* were collected (working upstream to T8) in glass bottles sterilised by autoclaving at 123 °C for 20 min. Care was taken not to disturb the channel bed to prevent contamination from *E. coli* stored in the sediment. Samples were placed in cool boxes until processing began within 6 h of collection. Concentrations of *E. coli* were determined using the Colilert-18 most--probable-number (MPN) method (IDEXX Laboratories, Westbrook, Maine, USA). Samples were well-shaken to ensure uniform distribution of *E. coli* prior to 100 ml being decanted to provide concentrations in MPN 100 ml^{-1}. When high concentrations of *E. coli* were likely, dilutions were made using sterile Ringers' solution. The limit of detection for undiluted samples was 1 MPN 100 ml^{-1}. *E. coli* loads (MPN d^{-1}) were derived by multiplying observed concentrations of *E. coli* at the outlet, T6 and T8 by average daily discharge for each respective site.

Number and type of livestock in each agricultural land parcel of the catchment (Fig. 1c) was recorded each sampling day. Where a land parcel represented a field with boundaries that extended beyond the Tulloch Burn catchment, the total number of livestock in the whole field was scaled by the fraction of the field falling within the land parcel. This assumed livestock would be uniformly distributed within a given field (c.f. Dorner et al., 2006; Haydon and Deletic, 2006). If livestock could move between land parcels, then the total number of livestock in all connected parcels was counted and scaled to each individually based on the fraction of the total connected area they represented. In addition, whether gates prevented livestock access to the stream at crossing points DS1-3 (Fig. 1c) was also recorded. The remainder of the stream was either fenced off and inaccessible to livestock, or, for stream sections in Mid Pastures (L) and (R), permanently open to livestock (Fig. 1c and e). Daily timeseries of stream access and livestock counts were generated from the twice-weekly observations by assuming any changes occurring between successive observation days did so at the mid-point between them.

3.3. Setup of EcH$_2$O-iso for the Tulloch Burn

In EcH$_2$O-iso, the spatial grid for simulations is defined by a digital elevation model (Kuppel et al., 2018a). A 5 × 5 m resolution LandMap digital terrain model (DTM) was resampled to 30 × 30 m resolution for delineating the Tulloch Burn catchment and deriving local slopes and drainage directions. The relatively coarse spatial resolution was necessary to keep model runtimes manageable given the long spin-up period needed for simulated water ages to stabilise. Simulation of 22 years with a daily timestep was necessary, with the period 27/04/17 to 31/12/17 for the last year retained for further analysis. The 22-year spinup was achieved by looping meteorological and isotopic inputs for 2016–2017 eleven times (c.f. Hrachowitz et al., 2010). Meteorological data before establishment of a catchment weather station (October 2016) were derived from the adjacent Aboyne and Bruntland Burn stations using statistical relationships from periods of overlapping data, whilst radiation for all of 2016 was available from the ERA-Interim climate reanalysis. For altitudinal effects on precipitation and temperature, a 5.5% increase in precipitation (Ala-aho et al., 2017) and decrease of 0.6 °C (Goody and Yung, 1995) with every 100 m elevation gain was implemented.

Parameterisation of soil hydrological properties in EcH$_2$O-iso was based on the five mapped soil types in the catchment (Soil Survey of Scotland Staff, 2014, Fig. 1b). Soil properties were assumed to be uniform within each type. To facilitate parameterisation of vegetation, land parcels of the Tulloch Burn in Fig. 1c were divided into three categories: agriculture, forest and heather moorland. Based on local knowledge, agricultural areas were assumed to comprise 95% grass and 5% bare soil, forested land was assumed to comprise 68% conifers, 30% grasses and 2% bare soil, and heather moorland was assumed to comprise 95% heather and 5% bare soil. To identify parameters for calibration, an initial sensitivity analysis was undertaken following the method of Morris (1991) and Sohier et al. (2014) using eight trajectories and a radial step for evaluating the parameter space. This identified 11 soil-related, 13 vegetation-related and two channel-related parameters as sensitive (Table S1), resulting in the need to calibrate 96 individual parameter values ([11 × 5]+[13 × 3]+2 = 96). Values of fixed parameters are given in Table S2.

3.4. Multi-criteria calibration of EcH$_2$O-iso

Calibration of the 96 parameter values followed a multi-criteria approach incorporating stream discharge (outlet) and δ^2H (outlet + sites T2-8) as calibration targets. Latin Hypercube Sampling was used to generate 100,000 parameter sets for EcH$_2$O-iso, based on the sampling ranges given in Table S1. For each model run, mean absolute errors (MAEs; Willmott and Matsuura, 2005) were calculated to quantify the skill of the run in simulating the dynamics of each calibration target for the period 27/04/17 to 31/12/17. For discharge, use of MAE avoided overemphasis on high-flows typical of alternatives such as the Nash-Sutcliffe efficiency statistic (Krause et al., 2005; Legates and McCabe, 1999), whilst for isotopes the limited variability in observations and daily timestep of the model necessitated use of a measure of average error (c.f. Gupta et al., 2009; Schaefeli and Gupta, 2007). A single performance metric for each model run was then derived by combining MAEs for individual calibration targets via a weighted-addition (e.g. Beven, 2012). This allowed the number of observations for each calibration target to determine the influence of its associated MAE in defining overall performance of the run and enabled identification of a "best" run for use in providing the hydrological environment for MAFIO (Section 3.5.2).

As MAE is dimensional with an optimal value of 0, it was necessary to convert the MAEs associated with each calibration target into dimensionless metrics that monotonically increase with model performance, prior to implementing the weighted addition. The latter need was met by calculating the metric (1-MAE), which increases with model performance to an optimum of 1 (in both instances 1 is in units of the calibration target). To remove dimensionality and obtain a metric (*MAE**) for use in the weighted addition, the following equation was applied:

$$MAE^*_{i,j} = \frac{(1 - MAE_{i,j}) - \min(1 - MAE)_j}{\max(1 - MAE)_j - \min(1 - MAE)_j} \quad (2)$$

where $MAE_{i,j}$ is the MAE associated with calibration target j for model run i and $(1\text{-}MAE)_j$ is the complete set of (1-MAE) associated with calibration target j from all 100,000 model runs. For a given run, a final goodness of fit in the range [0,1] was obtained through the weighted addition:

$$GOF_i = \sum_{j=1}^{n} W_j . MAE^*_{i,j} \quad (3)$$

where GOF_i is the goodness of fit value of run i and W_j is the weighting given to the performance metric *MAE** associated with calibration target j. The weighting of a performance metric associated with a given calibration target was the fraction of observations for all calibration targets that it contained. Numbers of observations and consequent weightings for each target used in the calibration are detailed in Table 1. Following calibration, an ensemble of the 100 model runs with the highest *GOF* values (behavioural runs) were retained to examine model performance and uncertainty.

3.5. Setup of MAFIO for the Tulloch Burn

As a first test of the model, MAFIO was used to simulate the behaviour and transport of *E. coli* in the Tulloch Burn during the MOP. This section describes the setup of the catchment and hydrological environments of the model (see Section 3.2 of Neill et al., 2020) and its

Table 1
The number of observations for each calibration target and the weighting for each target in the multi-criteria calibration.

Dataset	Number of observations	Calibration weighting
Discharge: Outlet	249	0.396
Isotopes: Outlet	242	0.385
Isotopes: T2	16	0.025
Isotopes: T3	16	0.025
Isotopes: T4	16	0.025
Isotopes: T5	16	0.025
Isotopes: T6	28	0.045
Isotopes: T7	16	0.025
Isotopes: T8	29	0.046
Total	628	1.0

parameterisation for *E. coli*.

3.5.1. Catchment environment

Table 3 of Neill et al. (2020) outlines the inputs necessary to characterise the catchment environment. Catchment extent and local drainage directions were defined from the 30 × 30 m DTM (identical to EcH$_2$O-iso). The spatial distribution of land parcels and of cells containing degraded soil/the channel were defined as shown in Fig. 1c. To facilitate representation of sub-grid heterogeneity in the latter, channel widths were derived from linear interpolation between field measurements of bankfull width. In addition, land parcels either adjacent to the stream (stream-associated land parcels) or from which livestock could contribute to soil degradation were defined as those falling within the 30 × 30 m footprint of a given cell as determined from field observations and aerial imagery (Table S3). The cell(s) immediately upslope of those containing degraded soil/the channel were defined from local drainage directions (Fig. S1). Timeseries of livestock counts and access to the stream were as described in Section 3.2.

3.5.2. Hydrological environment

The hydrological environment of MAFIO was simulated by the "best" overall ensemble run of EcH$_2$O-iso. To qualitatively assess the potential for uncertainty in the outputs of EcH$_2$O-iso to impact MAFIO simulations, spatial patterns of surface and groundwater flow paths and soil saturation deficit simulated over the MOP by the "best" run and by the 100 behavioural runs were compared. This indicative approach was taken as a full quantitative uncertainty analysis would require using the 100 behavioural EcH$_2$O-iso runs to generate the hydrological environment for an ensemble of MAFIO runs, the latter necessary to account for the effect of stochasticity (see Section 3.6). Such an uncertainty analysis was beyond the scope of this initial proof-of-concept test of MAFIO; however, this will be a focus of future work. To aid in assessing process representation in MAFIO, the simulated hydrological environment was characterised by generating spatial summaries of discharge, δ^2H and water ages in the stream, and of overland flow, soil saturation deficit and groundwater fluxes within the catchment, for the whole MOP and for exemplar "dry" (10/08/17) and "wet" (15/08/17) days. Here, stream-water ages denote how long water contributing to discharge spent travelling through the catchment since entering it as precipitation (Sprenger et al., 2019).

3.5.3. Parameterisation of MAFIO sub-models

Parameter values for the MAFIO sub-models are presented in Table 4 of Neill et al. (2020). Sheep and cattle were the only livestock reared in the catchment. Most parameter values were taken from the extensive literature on *E. coli* as an FIO. Exceptions were the parameters *faecesConc* (concentration of FIOs in livestock faeces) and *agentsRepresent* (number of FIOs shed in reality for which an FIO-agent is introduced into the simulation). For the former, geometric mean concentrations of *E. coli* in sheep and cattle faeces were determined from faecal samples collected in the catchment during 2017 and 2018 (Avery et al., *unpublished data*). Meanwhile, the minimum value of *faecesConc* was used for *agentsRepresent* (i.e. 4.18×10^5 MPN FIO-agent^{-1}). This was the minimum permissible value given available computational resources; however, similarities between simulations obtained using this value and a value of 1×10^8 MPN FIO-agent^{-1} (*Data not shown*) suggested that significant changes to model outputs would be unlikely if a smaller value were to be used. This provided confidence that a sufficient quantum of *E. coli* was simulated by MAFIO. Despite potential uncertainty in the values of model parameters (Oliver et al., 2016), calibration was not undertaken in this initial application. This was primarily because use of stochasticity to model processes conceptualised in ABMs hinders the use of "fit-to--data" metrics (i.e. those quantifying model skill in reproducing dynamics of observed data) often used in automated calibration (Polhill and Salt, 2017). This is further described in Section 3.6. A benefit to using the model uncalibrated is that it offers insight into the process consistency of the model if physically-meaningful parameter values are used (c.f. Kuppel et al., 2018a), as compensatory parameter effects on model structural deficiencies from calibration are avoided (c.f. Beven, 2019).

3.6. Application of MAFIO

MAFIO was applied for the MOP on a 30 × 30 m spatial grid using a daily time step, consistent with the spatio-temporal resolution of data characterising the catchment and hydrological environments. For initialisation, values for the fraction of damaged soil (*dFrac*) at DS1, DS2 and DS3 were set to 0.72, 0.53 and 0.7155, respectively, based on application of Eq. 3 of Neill et al. (2020) with livestock counts made in the catchment since 01/01/17. As these counts also showed all pasture land parcels to have been grazed to some extent since the start of 2017, all were set to have FIO-agents already in the soil at initialisation as a significant soil reservoir of *E. coli* may persist for several months even after cessation of grazing (Muirhead, 2009). Initial numbers of FIO-agents were based on estimates of the total number of *E. coli* in the upper soil of each land parcel (between 4.1×10^9 and 9.3×10^{10} *E. coli*). These were approximated from concentrations of *E. coli* (in MPN g^{-1}) measured in the top 5 cm of soil at five locations within the Lower and Mid Pasture fields (Avery et al., *unpublished data*) and estimates of the mass of soil in each land parcel over the same depth.

An ensemble of 30 model runs using the same parameterisation and input was made for the MOP to characterise stochastic variability in MAFIO outputs (Abdou et al., 2012). Combined with the fact that natural variability intrinsic to complex systems can cause observed data to be conditional on a particular trajectory having been taken by the system, of which many may have been possible (Refsgaard et al., 2007; Windrum et al., 2007), this stochastic variability characteristic of ABM outputs can complicate assessments of model performance (Brown et al., 2005). In particular, traditional "fit-to-data" metrics become inappropriate as exclusive means of evaluating ABM performance as a model that adequately represents the processes giving rise to observations could be unfairly penalised if, due to stochastic treatment of system processes, it simulates a range of plausible scenarios which may or may not include what was observed (Polhill and Salt, 2017). Whilst a "benchmark" alternative is yet to emerge, other ABM work has highlighted the value of combining quantitative performance evaluation with qualitative "checks" that focus on understanding how simulated characteristics at larger scales emerge from the processes influencing the behaviour of individual agents and assessing the plausibility of such processes similarly effecting the phenomena under investigation in reality (Moss and Edmonds, 2005; Polhill et al., 2010; Polhill and Salt, 2017).

Consequently, the following approach to performance assessment was adopted. For each ensemble run, observed and simulated *E. coli* loads were compared quantitatively at the outlet, T6 and T8. Since MAFIO simulates fluxes of FIO-agents, simulated loads were approximated by multiplying FIO-agent fluxes by the value of *agentsRepresent*.

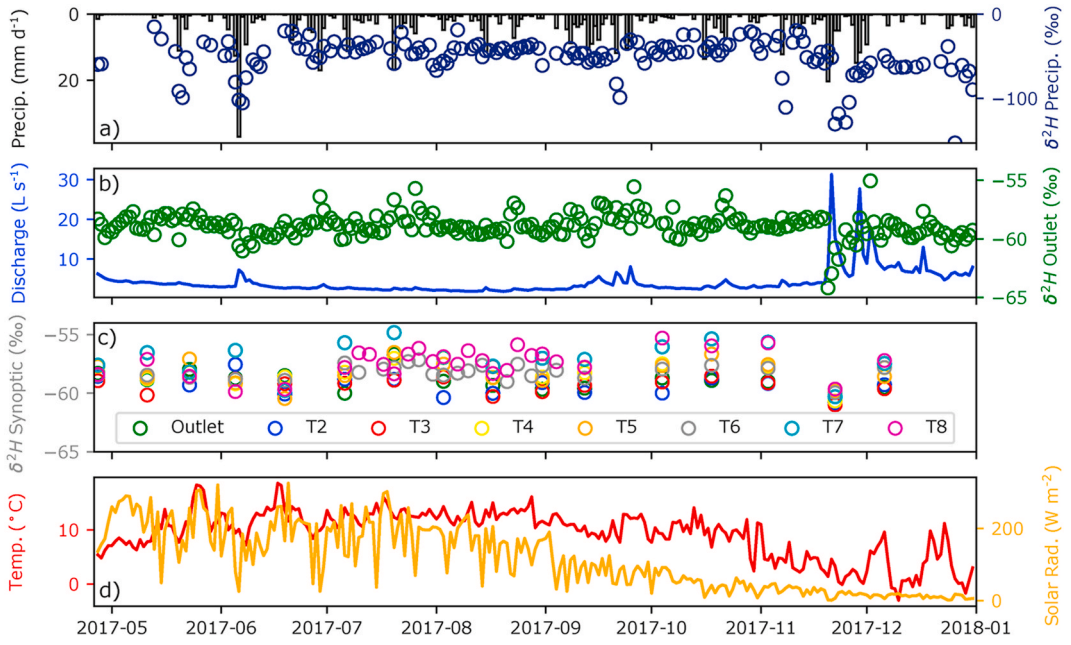

Fig. 2. For the full study period, observed timeseries of a) Precipitation and its associated isotopic composition; b) Daily average discharge at the catchment outlet and its associated isotopic composition; c) Isotopic compositions of streamwater at synoptic sampling sites; d) Daily average temperature and solar radiation.

As this parameter dictates the precision to which observed loads can be simulated (c.f. Parry and Bithell, 2012), the skill of MAFIO in capturing periods of relatively more or less impaired microbial water quality was also assessed (c.f. Oliver et al., 2010; Porter et al., 2017). This was achieved by calculating Z-scores showing the number of standard deviations an observed *E. coli* load or simulated flux of FIO-agents was away from the mean of its associated timeseries. As observations were not available for all dates, Z-scores for simulated FIO-agent fluxes were based only on simulations that overlapped with observations. Spearman's rank correlation coefficients were also used to assess how well MAFIO captured the relative order of observed *E. coli* loads at each site (c.f. Porter et al., 2017). For a qualitative "check" on the model, the plausibility of simulated outputs given the potential processes influencing *E. coli* dynamics in the Tulloch Burn was the subject of a literature-based discussion (Section 5.1) that also considered the performance of EcH_2O-iso in simulating the hydrological environment. Whilst such qualitative evaluation is less robust than alternative methods based on consultation of independent experts (e.g. Moss and Edmonds, 2005; Polhill et al., 2010), the latter was beyond the scope of this initial MAFIO application.

As a basis for assessing the potential of MAFIO in providing insights relevant to management, the overall flux of FIO-agents leaving the catchment in the stream ("exported FIO-agents") was observed and further disaggregated into contributions from different livestock types and transfer mechanisms. The latter were derived from the attributes *Domain type memory* and *Livestock type* (see Table 2 of Neill et al., 2020) of exported FIO-agents. By observing the *Location memory* attribute, areas where exported FIO-agents entered the stream via direct deposition and pathways taken by exported FIO-agents reaching the stream in overland flow or seepage were also identified. For each timestep, pathways were derived by quantifying the total number of exported FIO-agents that had passed through each grid cell in overland flow or seepage at any point whilst being transported from their original spawning location to the stream (i.e. pathways reflect the transport of exported FIO-agents over their entire existence, not just during the timestep in which they were exported). Meanwhile, spatial patterns of direct deposition were characterised by quantifying the total number of exported FIO-agents entering the stream via direct deposition for each cell containing a channel. For each of the 30 ensemble runs of MAFIO, timestep totals were extracted for the example dry and wet days and further summed over the whole MOP. Median totals for each cell across the ensemble runs were then used to generate "average" maps of direct deposition and pathways taken to the stream by exported FIO-agents for each period of interest, whilst maps using ranges in totals were generated to evaluate the effect of stochastic variability in ensemble simulations.

4. Results

4.1. Hydrometric and isotope observations

Hydroclimatic conditions in 2017 were typical for the region (Hannaford et al., 2018). The study period started out relatively dry, with only 23 mm of precipitation falling by the end of May (Fig. 2a). Consequently, summer baseflows were established by mid-June (Fig. 2b), despite the largest precipitation event of the study (37.2 mm d^{-1}) occurring at the beginning of that month, two days before the MOP commenced. For the remaining summer, precipitation fell in low-intensity events that generated small discharge responses (Fig. 2a–b and 3a). Sustained periods of precipitation in mid-September re-wetted the catchment leading to a rise in baseflows and the largest discharge responses (up to 31 L s^{-1}) being observed in November (Fig. 2a–b).

The δ^2H composition of precipitation ranged between −153.1‰ and −14.9‰ (Fig. 2a). By contrast, the δ^2H composition of stream water at the outlet was substantially damped (range −64.2‰ to −55.0‰), though deviations in the direction of the precipitation signal were observed during events (Fig. 2b). At T2-8, δ^2H was similarly damped, ranging between −61.0‰ and −54.8‰ across all sites (Fig. 2c). These sites behaved similarly to the outlet in terms of variability; however, the upper T7 and T8 sites had slightly more enriched δ^2H values, with values then becoming more depleted towards the outlet (Fig. 2c). Daily average air temperatures peaked at ~18 °C in May and June and fluctuated ~12 °C until September when temperatures fell towards a minimum of −3 °C in December (Fig. 2d). Solar radiation followed a similar trajectory (Fig. 2d).

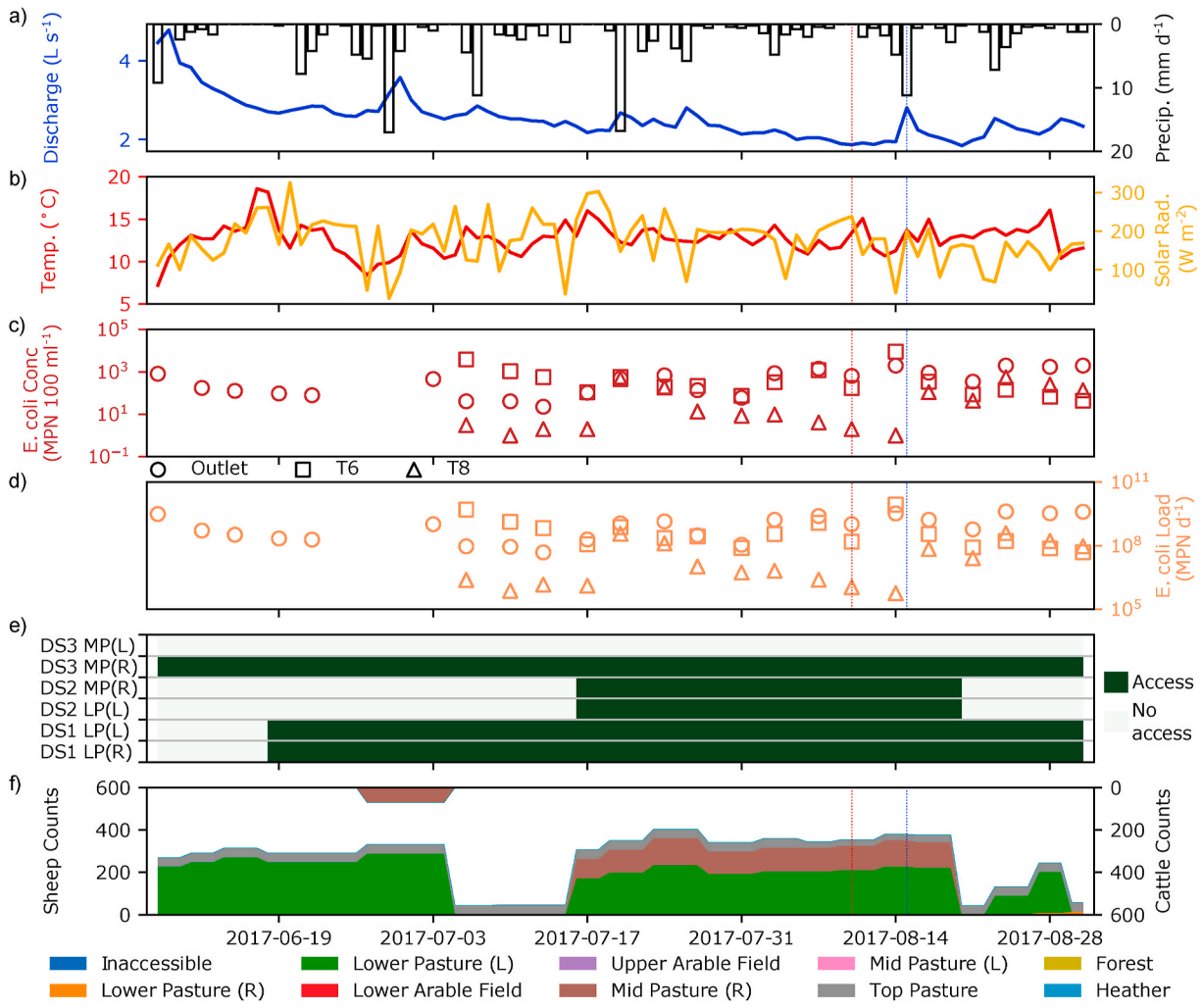

Fig. 3. For the microbial observation period, timeseries of observed a) Precipitation and daily average discharge at the catchment outlet; b) Daily average temperature and solar radiation; c) Concentrations of *E. coli* (plotted on a log scale); d) *E. coli* loads (plotted on a log scale); e) Accessibility of the stream to livestock at the discrete crossing points (DS1-3 in Fig. 1c); f) Sheep and cattle counts. The red and blue dashed lines denote the example dry and wet days, respectively. In (c) and (d), MPN = most-probable-number. In (e), the abbreviations LP and MP refer to Lower Pasture and Mid Pasture, respectively. (For interpretation of the references to colour in this figure legend, the reader is referred to the Web version of this article.)

4.2. Microbial observation period (MOP)

Microbial observations began as the hydrograph experienced a small secondary peak in response to precipitation that occurred following the 37.2 mm d^{-1} precipitation event (Fig. 2a–b and 3a). Peak daily average temperature and solar radiation for the overall study period fell within the MOP, with the former averaging 12.7 °C and the latter 176 W m^{-2} (Fig. 3b).

Table 2
The mean absolute error (MAE) for simulations of discharge and isotope data by the "best" run of EcH$_2$O-iso (Best MAE), and summary statistics for simulations by the 100 behavioural runs.

Dataset	Best MAE	Mean MAE	Min - Max MAE
Discharge: Outlet	1.37 L s^{-1}	1.56 L s^{-1}	1.24–2.04 L s^{-1}
Isotopes: Outlet	1.41‰	1.99‰	1.12–3.68‰
Isotopes: T2	1.30‰	2.06‰	1.02–3.82‰
Isotopes: T3	1.14‰	2.13‰	0.95–3.82‰
Isotopes: T4	2.73‰	3.57‰	0.83–6.20‰
Isotopes: T5	2.69‰	3.56‰	1.00–6.25‰
Isotopes: T6	2.00‰	3.36‰	0.86–6.51‰
Isotopes: T7	3.02‰	4.64‰	1.55–8.21‰
Isotopes: T8	2.52‰	4.23‰	1.30–8.08‰

Temporal dynamics of *E. coli* concentrations and loads at individual sites were similar (Fig. 3c–d). At the outlet, concentrations ranged from 2.3×10^1 to 2.0×10^3 MPN 100 ml^{-1} (Fig. 3c), whilst loads varied between 4.9×10^7 and 4.1×10^9 MPN d^{-1} (Fig. 3d). Both were highest towards the end of the MOP and lowest during early July. The latter coincided with no livestock present in fields closest to the catchment outlet (Figs. 1c and 3f), suggesting that this period may have been characterised by background concentrations of *E. coli*. At T6, concentrations and loads varied between 4.4×10^1 and 9.1×10^3 MPN 100 ml^{-1} and 5.0×10^7 and 8.7×10^9 MPN d^{-1}, respectively (Fig. 3c–d). Thus, whilst T6 and the outlet generally experienced similar concentrations and loads of *E. coli*, these could be higher at the former site. T8 was generally the least-contaminated site as concentrations of *E. coli* were <10 MPN 100 ml^{-1} on over half the sampling days (Fig. 3c). However, higher concentrations on the order of 10^2 MPN 100 ml^{-1} were also observed, most frequently towards the end of the MOP. Loads varied between 5.8×10^5 and 3.9×10^8 MPN d^{-1} (Fig. 3d) and were, consequently, often much smaller than loads observed at the outlet and T6 (exceptions are the last three sample dates of the MOP where loads at T8 were greater than at T6). A clear response of *E. coli* concentrations and loads to discharge was elusive; however, a link to livestock counts was more apparent at the outlet and T6.

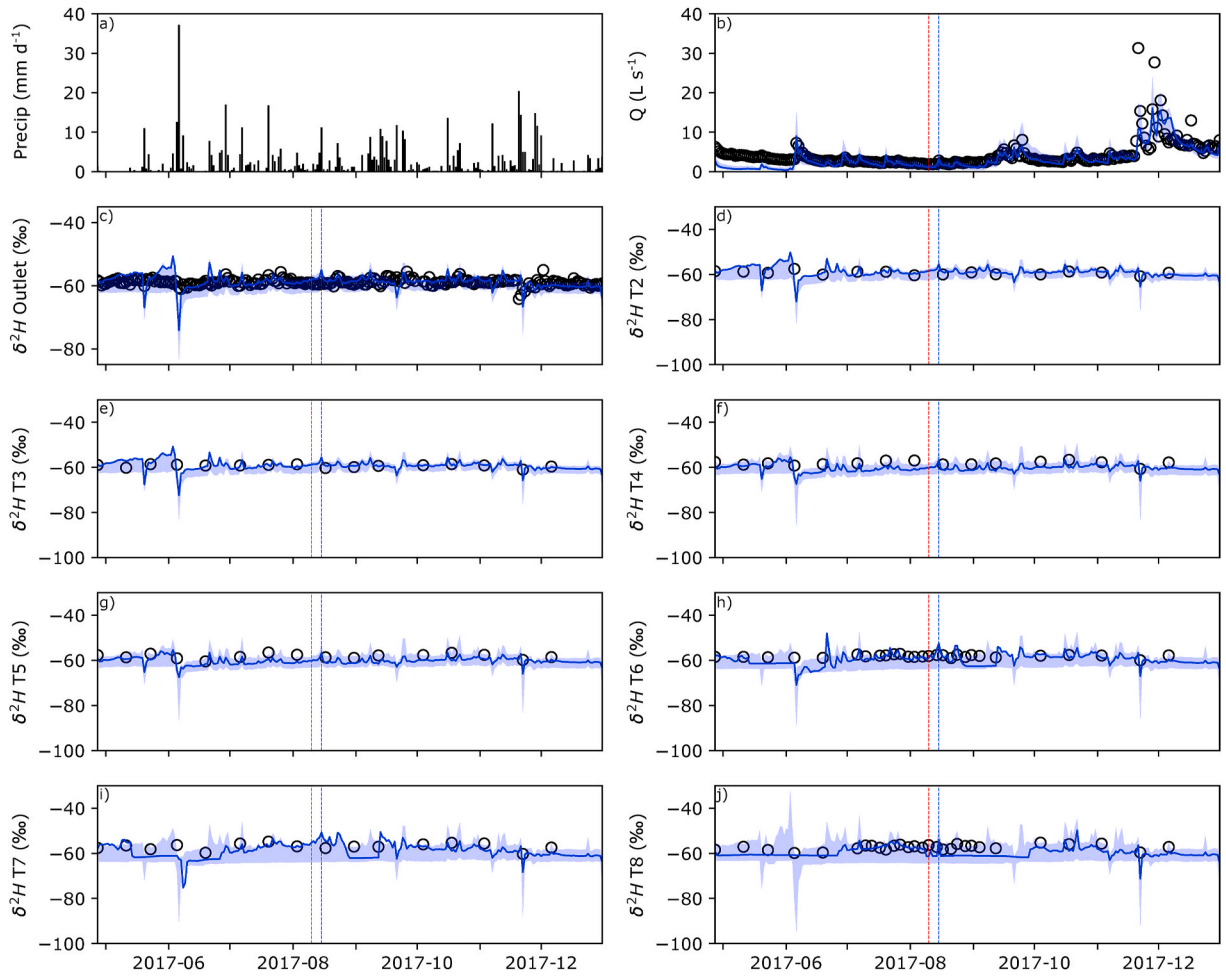

Fig. 4. Timeseries of a) Precipitation; b) Observed and modelled discharge at the catchment outlet; c-j) Observed and modelled isotopes at the catchment outlet and synoptic sampling sites. Shaded areas show the 90% spread of simulations from the behavioural ensemble, whilst the solid blue line shows the "best" simulation. The red and blue dashed lines denote the example dry and wet days, respectively. Note the different y-scales between isotope data for the outlet (c) and for the synoptic sampling sites (d–j), necessary to show the greater spread of the simulations for the latter. (For interpretation of the references to colour in this figure legend, the reader is referred to the Web version of this article.)

Timeseries showing stream accessibility to livestock at the three discrete crossing points are shown in Fig. 3e. Sheep were the main livestock in the catchment and were in Lower Pasture (L), Mid Pasture (R), Top Pasture or, for a short time late in the MOP, Lower Pasture (R) (Fig. 3f). Cattle were briefly present in Mid Pasture (R) from late June to early July (Fig. 3f).

4.3. Multi-criteria calibration of EcH$_2$O-iso

The results of calibrating EcH$_2$O-iso to discharge and spatially-distributed isotope data are summarised in Table 2 and Fig. 4; calibrated parameter ranges are given in Table S1. Discharge was generally well-simulated (Table 2), with behavioural model runs successfully capturing the summer baseflows and small events that characterised the MOP alongside the re-wetting of the catchment in September and timing of the largest discharges in November (Fig. 4b). The magnitudes of the latter were, however, under-estimated, as were discharges at the start of the simulation period (Fig. 4b). For isotopes, the model could reproduce the markedly-damped composition of streamwater at the outlet (Table 2; Fig. 4c). Isotopic variability in response to precipitation was also generally well-captured, though more extreme excursions could be simulated. Skill in simulating isotope dynamics at the synoptic sampling sites was more variable (Table 2; Fig. 4d–j), likely reflecting their lower weighting in the multi-criteria calibration (Table 1) and the sparser temporal resolution of observations. Performance was best for sites closer to the outlet, whilst simulations for sites further upstream showed greater uncertainty with some ensemble runs exhibiting poorer performance. However, performance was still maintained in the "best" overall run, with MAEs not exceeding ~3‰ at the upstream sites (Table 2). Overall, it was encouraging that EcH$_2$O-iso generally reproduced the damped isotope signals observed at the synoptic sampling sites.

4.4. Characterisation of the hydrological environment

Median discharges over the MOP (Fig. 5a) simulated by the "best" run of EcH$_2$O-iso decreased in age with distance downstream (Fig. 5e) but did not exhibit a clear spatial pattern in δ^2H (Fig. 5c). Median streamwater ages were relatively old (averaging ~1.5 years), reflecting the dominant simulation of groundwater fluxes over surface water fluxes. Overland flow was only simulated for very restricted areas, mainly limited to stream-proximal cells in the lower part of the catchment (Fig. 5b). Over the MOP, cells for which overland flow was simulated generated total fluxes <1000 mm. By contrast, simulated groundwater fluxes over the MOP could be up to 4700 mm for individual cells and occurred across much of the catchment (Fig. 5f). The limited extent of simulated overland flow arose from much of the soil in the catchment being in saturation deficit (Fig. 5d). Highest deficits were generally simulated in the upper catchment in areas of forest and

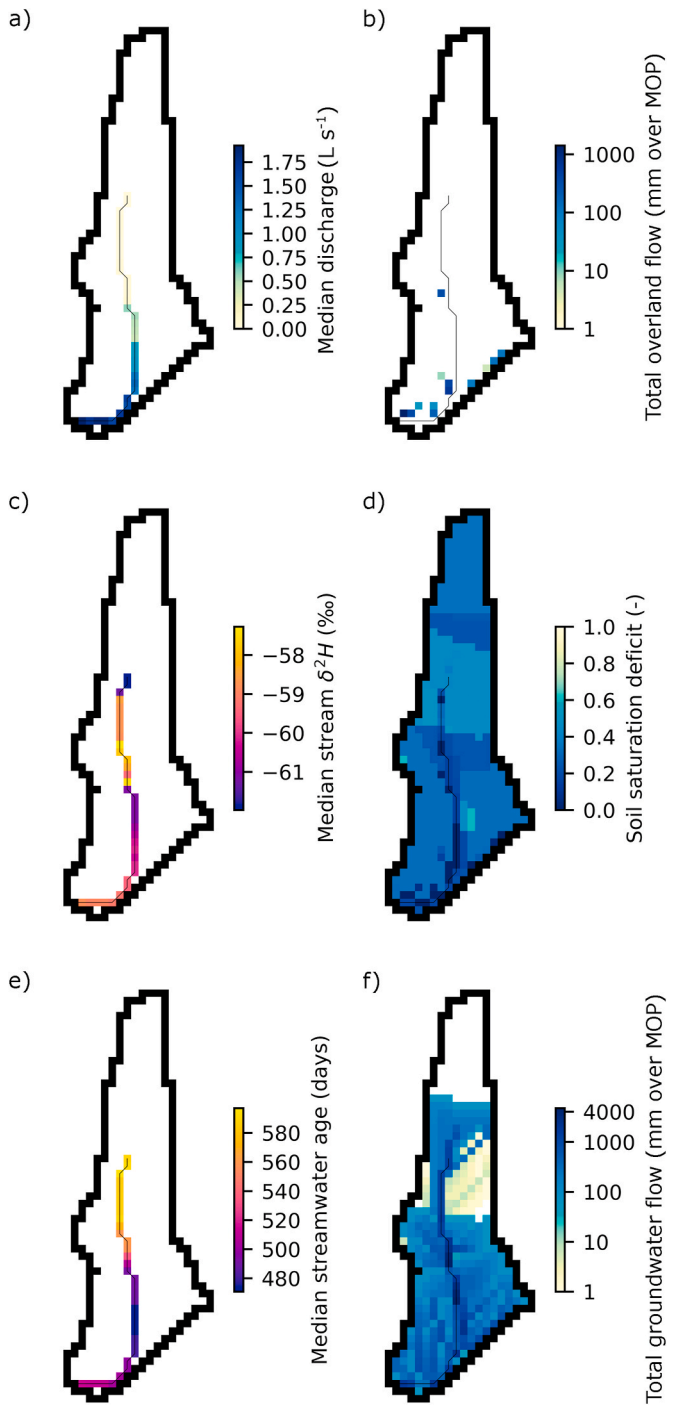

Fig. 5. Maps showing for the microbial observation period a) Median stream discharge; b) Total overland flow; c) Median stream δ^2H; d) Median soil saturation deficit; e) Median streamwater age; f) Total groundwater flow, based on the "best" ensemble run of EcH$_2$O-iso. Overland (b) and groundwater (f) flows are plotted on log scales for clarity, with areas of white denoting fluxes of 0. MOP = Microbial observation period.

heather (Fig. 1c) underlain by podzolic soils (Fig. 1b); here, overland and groundwater fluxes were consequently minimal (Fig. 5b and f).

Stream discharges simulated for the example wet day were higher than for the dry day (Fig. 6a) and consisted of younger water (median age of streamwater 399 days vs. 522 days; Fig. 6e). The isotopic composition of the stream was also generally more enriched in wet conditions (Fig. 6c). This, together with the lower streamwater ages, indicates increased contributions of younger overland flow and soil water to streamflow during summer wet conditions compared with the dominance of older groundwater during drier periods. However, even when wet, overland flow remained spatially limited, with just a few cells adjacent to the stream and a small number of distal, unconnected cells simulating fluxes of up to 35.3 mm d^{-1} (Fig. 6b). In dry conditions, overland flow was generated from more restricted areas that maintained saturation by virtue of their position in flatter parts of the riparian area (Fig. 6b). Overland flow was limited due to most soil being in saturation deficit in both dry and wet conditions (Fig. 6d). In contrast, groundwater fluxes were active across similar spatial areas on the wet and dry days, with fluxes of up to 57.8 mm d^{-1} and 35.7 mm d^{-1} simulated for each day, respectively (Fig. 6f).

Assessment of the spatial outputs from the 100 behavioural runs of EcH$_2$O-iso revealed that generation of overland flow from areas proximal to the stream and the dominance of groundwater simulated by the "best" run was also simulated with reasonable certainty (i.e. in >50% of runs) by the ensemble (Fig. 7a–c). In addition, relative spatial patterns of moisture deficits were comparable (Fig. 7d). However, it was possible for some behavioural runs to simulate larger areas of overland flow generation, leading to uncertainty in the exact spatial extent of surface flow paths (Fig. 7c). The implications of this will be discussed with respect to assessing the adequacy of process conceptualisation in MAFIO.

4.5. Performance of MAFIO

Simulated *E. coli* loads at the outlet captured the main dynamics of observations quite well; in particular, the observed decrease in loads in early July and subsequent increase, relatively constant loads in early-to mid-August, and brief dip in loads towards the end of the MOP were all simulated (Fig. 8a). However, there was a general tendency for loads to be over-predicted, with the main exceptions being at the end of the MOP and when observed loads decreased in July (Fig. 8a). Z-scores at the outlet show that the model was more successful in capturing when loads were above- and below-average, with the sign of the Z-scores simulated correctly in the majority of cases (Fig. 8b). Exceptions were at the end of the simulation (reflecting over-prediction of observed loads earlier on despite absolute loads at the end of the MOP being successfully captured) and on 03/07/17. Spearman's rank correlations ranged between 0.21 and 0.30 with an average of 0.26 across the 30 ensemble runs. Stochastic variability in outlet simulations was minimal (Fig. 8a–b).

At T6, all ensemble runs simulated loads of zero and Z-scores below 0 whenever livestock were absent from Mid Pastures (R) or (L) (Figs. 3f and 8c-d). Non-zero loads were only simulated when Mid Pasture (R) had livestock present (Figs. 3f and 8c); however, simulated loads and Z-scores exhibited a high degree of stochastic variability (Fig. 8c–d). Consequently, Spearman's rank correlations varied between runs, ranging from −0.12 to 0.32. When livestock were present in Mid Pasture (R), observations generally fell within simulation bands; however, loads were under-estimated when livestock were absent (Figs. 3f and 8c). For relative performance, observed Z-scores were often within the range simulated (Fig. 8d). When non-zero loads were simulated, the large range in simulated Z-scores meant that MAFIO was not consistent between ensemble runs in terms of simulating loads above- or below-average. At the end of the period, observed and simulated Z-scores were similar, suggesting that MAFIO successfully captured this as a time of relatively less-impaired microbial water quality.

Ensemble runs always simulated zero loads at T8 (Fig. 8e). Consequently, neither Z-scores for MAFIO simulations nor Spearman's rank correlations could be calculated. Qualitatively, the simulated behaviour was largely consistent with the low concentrations and loads of *E. coli* at T8 (Fig. 3c–d), and negative observed Z-scores (Fig. 8f). Quantitatively, however, the simulation of zero loads was not consistent with observations.

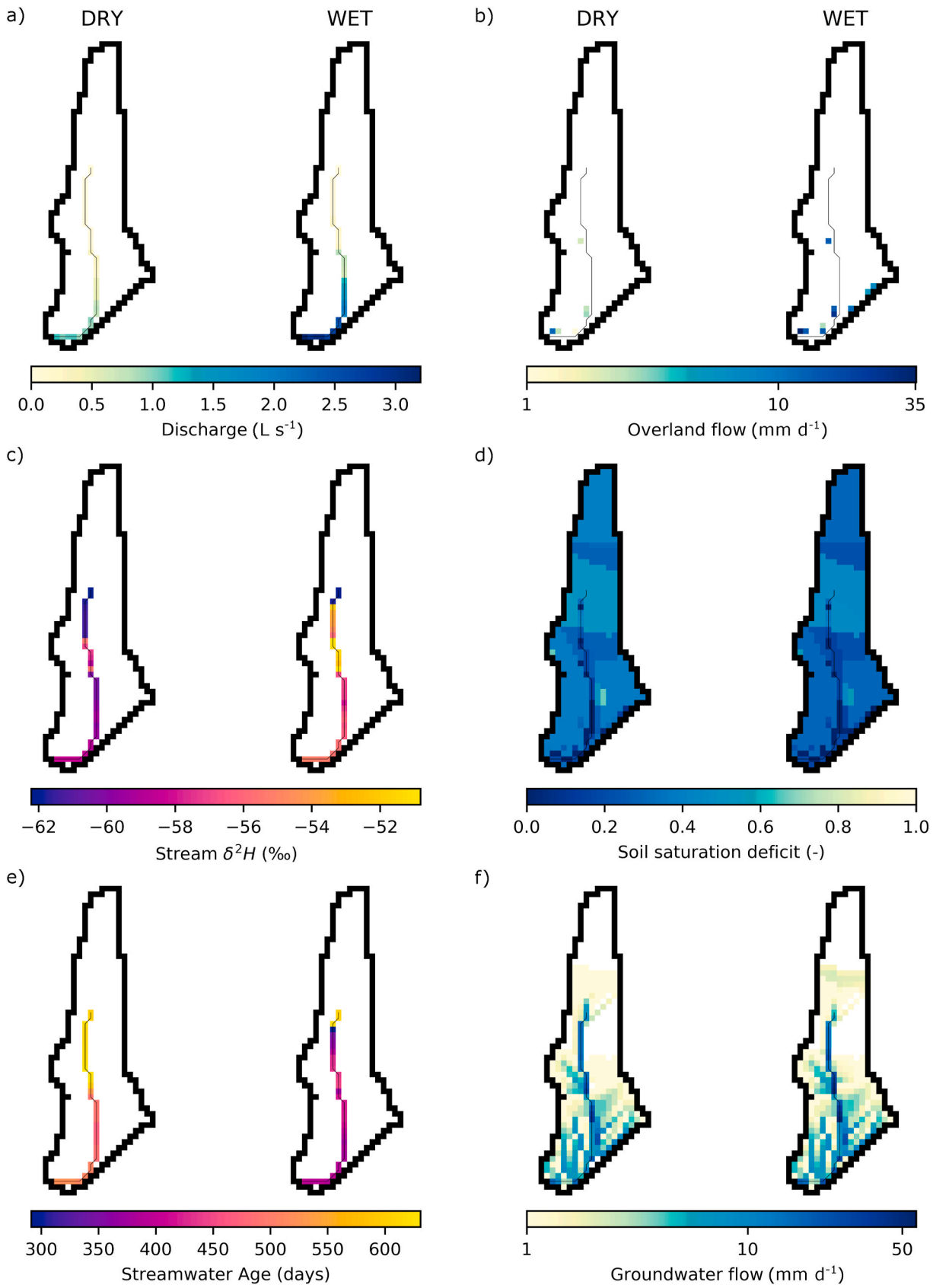

Fig. 6. For the example dry and wet days, maps showing a) Discharge; b) Overland flow; c) Streamwater δ^2H; d) Soil saturation deficit; e) Streamwater age; f) Groundwater flow, based on the "best" ensemble run of EcH$_2$O-iso. Overland (b) and groundwater (f) flows are plotted on log scales for clarity, with areas of white denoting fluxes of 0.

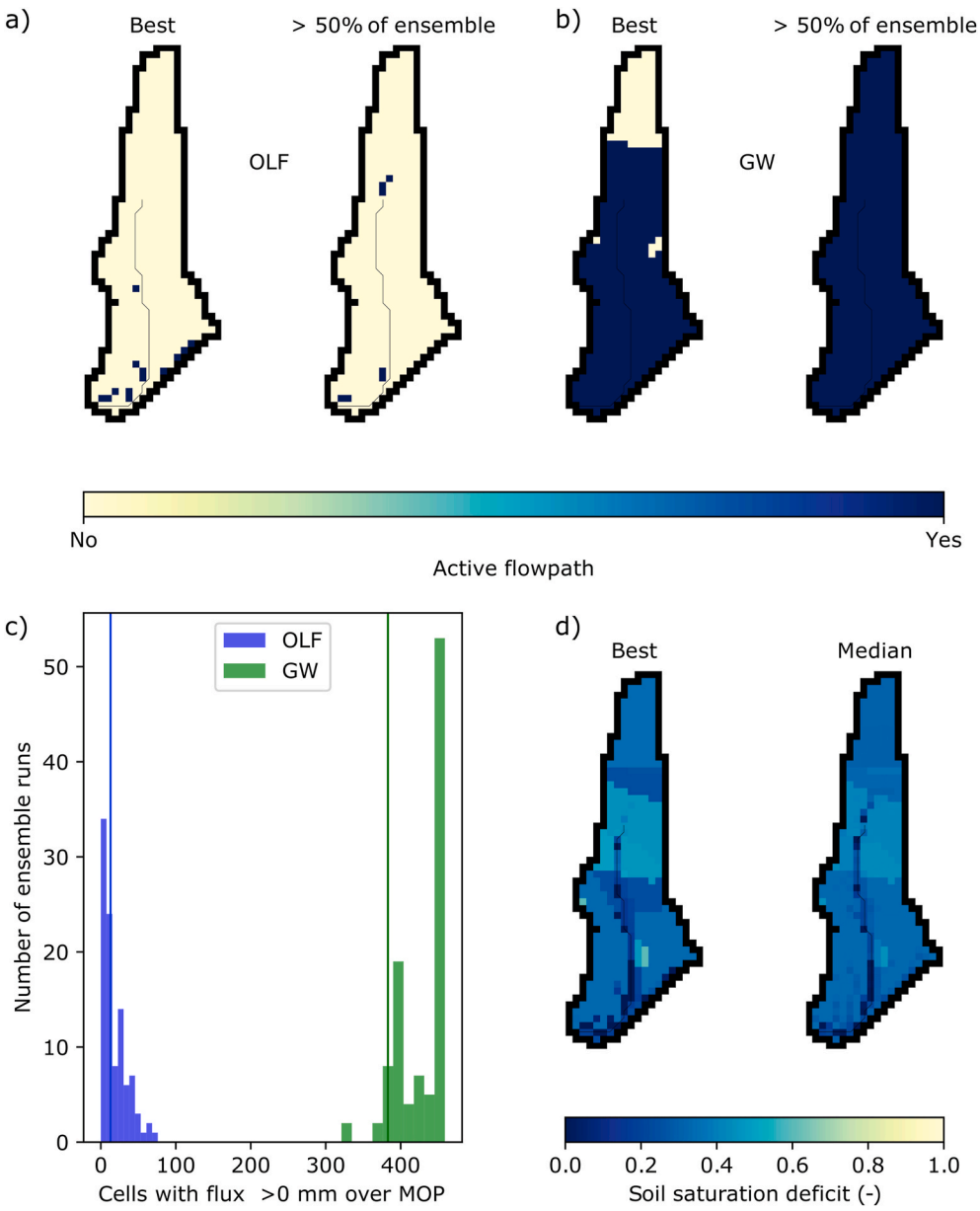

Fig. 7. Comparison of spatial simulations made by the "best" run of EcH_2O-iso and by an ensemble of 100 behavioural runs: a) Spatial extent of cells with total overland flow (OLF) fluxes greater than 0 mm over the microbial observation period (i.e. "Active flowpath") simulated by the "best" run and >50% of the ensemble; b) As (a) but for groundwater (GW); c) Histogram quantifying the number of ensemble runs in which different numbers of cells were simulated to have total OLF or GW fluxes greater than 0 mm over the microbial observation period (solid lines denote the "best" run); d) Spatial patterns of median soil saturation deficit over the microbial observation period simulated by the "best" run and of the median of the median deficits simulated by the behavioural ensemble. MOP = Microbial observation period.

4.6. *Sources and mechanisms contributing E. coli to streams*

To help interpret timeseries relating to exported FIO-agents, simulated effective precipitation, discharge at the outlet and storage of FIO-agents are shown in Fig. 9a–b. The simulated flux of exported FIO-agents (Fig. 9c) strongly reflected storage dynamics of FIO-agents (Fig. 9b) and livestock counts (Fig. 3f). Exported FIO-agents predominantly entered the stream via seepage from degraded soil (Fig. 9d) as simulated overland flow was limited (Fig. 5). When overland flow did transfer FIO-agents to the stream, localised spikes in export fluxes were simulated (Fig. 9c–d). Contributions were non-linear due to the changing storage of FIO-agents. When cattle were in Mid Pasture (R), both seepage and direct deposition made their greatest contributions of FIO-agents to the stream (Figs. 3f and 9d), reflecting the higher loading rates of *E. coli* from cattle (see Table 4 in Neill et al., 2020) and the extensive stream access in this field (Fig. 1c). Variability in flux magnitudes between ensemble runs was also greatest at this time (Fig. 9c). Contributions from direct deposition were otherwise minimal, reflecting the lower loading rates of sheep (see Table 4 in Neill et al., 2020) when present in Mid Pasture (R) or the limited number of discrete crossing points allowing stream access to livestock in other fields (Figs. 1c and 3e). Contributions from different livestock types largely corresponded to their presence in the catchment (Figs. 3f and 9e); however, a limited "memory-effect" in contributions reflected survival of FIO-agents in areas of degraded soil.

Over the MOP, similar median numbers of exported FIO-agents entered the stream via direct deposition wherever livestock were present with stream access (Figs. 1c, 3f and 10a). However, stochastic variability across the ensemble runs was evident (Fig. 10b). Pathways taken by exported FIO-agents reaching the stream in overland flow or seepage were constrained by the limited area over which the former was generated in the catchment (Figs. 5 and 10c). Fluxes of exported FIO-agents along individual pathways increased towards the stream with generation of overland flow (Figs. 5b and 10c); however, short pathways between areas of degraded soil and the stream were consistently followed by the largest numbers of exported FIO-agents (Figs. 1c and 10c). Overall, source areas contributing exported FIO-agents to the stream over the MOP were always restricted to stream-proximal locations (Fig. 10c–d). Stochastic variability in numbers of exported FIO-agents

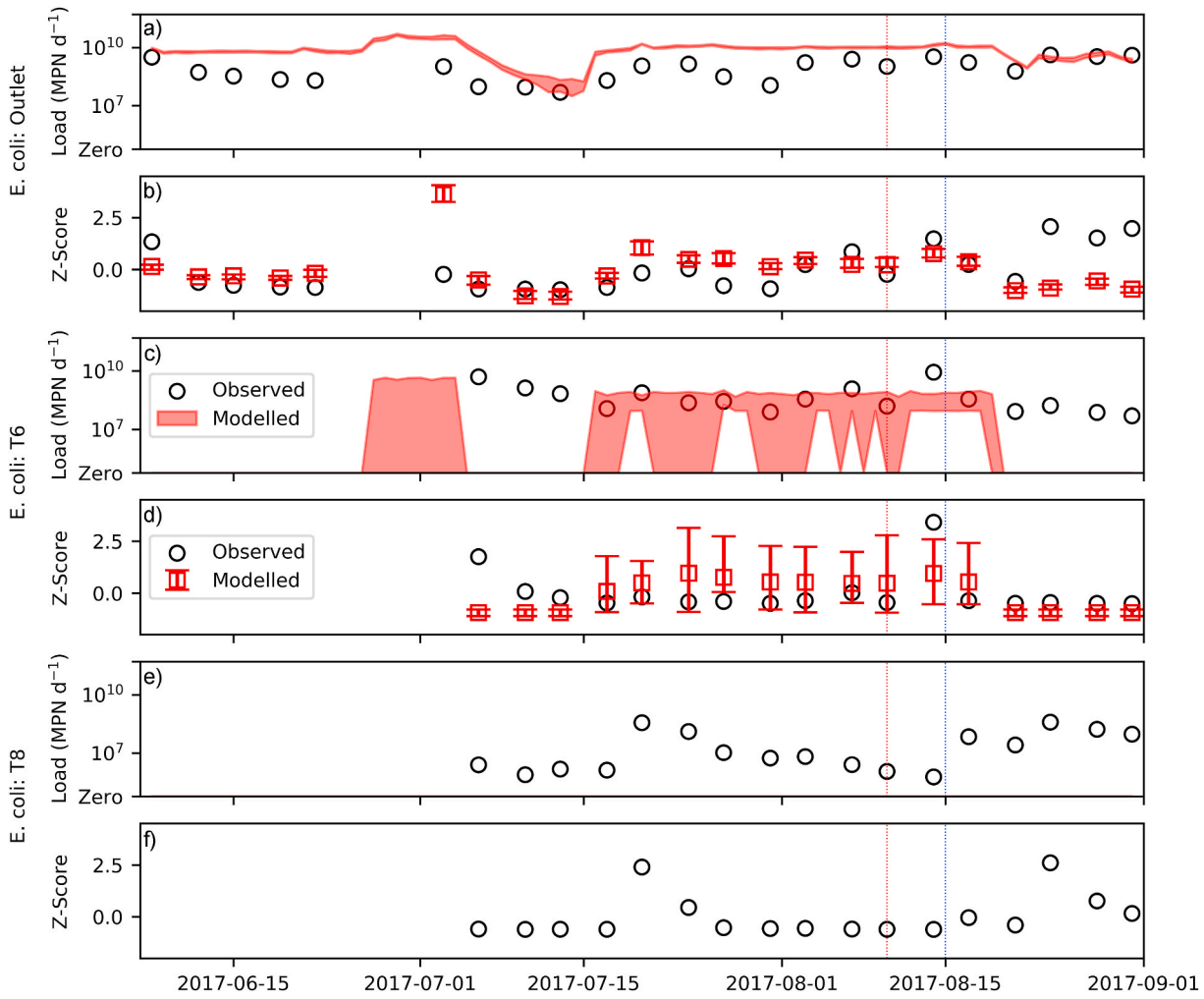

Fig. 8. Comparison of observed and simulated *E. coli* loads and Z-scores for a-b) The catchment outlet; c-d) T6; e-f) T8. In the latter, only observed Z-scores are given due to all ensemble runs of MAFIO simulating fluxes of zero FIO-agents for all timesteps. For modelled data, the square marker represents the median Z-score across the 30 ensemble runs of MAFIO, whilst the error bars/shaded areas denote the range of Z-scores/simulated loads. The red and blue dashed lines denote the example dry and wet days, respectively. Loads are plotted on a log scale - for presentational purposes, simulated loads of zero are set to plot along the lower limit of the y-axis (one order of magnitude below the minimum observed or simulated non-zero load across all sites). (For interpretation of the references to colour in this figure legend, the reader is referred to the Web version of this article.)

following particular pathways to the stream was usually less than for numbers being directly deposited in the stream (Fig. 10b and d).

On the example dry and wet days, there was a difference in the spatial distribution of cells for which the median number of exported FIO-agents entering the stream via direct deposition was non-zero (Fig. 11a and c). However, similar counts of sheep in Lower Pasture (L) and Mid Pasture (R) on both days (Fig. 3f) meant that when non-zero, median numbers were comparable (Fig. 11a and c). In addition, stochastic variability across ensemble runs showed that on either day, direct deposition of exported FIO-agents could occur wherever livestock had stream access (Fig. 11b and d). More extensive overland flow on the wet day (Fig. 6b) increased the spatial extent of pathways taken by exported FIO-agents to the stream, although contributing areas were always limited to near-stream locations (Fig. 11e and g). Fluxes of FIO-agents along individual pathways were elevated in wet conditions (Fig. 11g) due to the increased generation of overland flow (Fig. 6b). For both the dry and wet days, "average" maps indicated pathways taken by exported FIO-agents to the stream (Fig. 11e and g) that fully consisted of cells where overland flow was simulated (Fig. 6b) or seepage from degraded soil was possible (Fig. 1c). However, from considering the effect of stochastic variability between ensemble simulations (Fig. 11f and h), it is apparent that in some instances, exported FIO-agents had followed paths that included cells not hydrologically connected to the stream during the timestep in question (e.g. in Lower Pasture [L]; Figs. 1c and 6b). This indicates that FIO-agents previously moved and infiltrated into the soil could be exfiltrated and further transported. Stochastic variability in numbers of exported FIO-agents following particular pathways to the stream was generally lower overall for the dry event (Fig. 11f and h).

5. Discussion

5.1. To what extent does MAFIO resolve the main processes driving observed FIO dynamics?

Using models to explore issues of water quality, especially in a decision-making context, requires confidence that processes governing the determinand of interest are adequately captured (c.f. Vaché and McDonnell, 2006; Wellen et al., 2015). Consequently, the new agent-based model MAFIO was applied to the Tulloch Burn for a relatively data-rich period, in order to assess the adequacy of process representation in the model. The spatially-distributed, tracer-aided ecohydrological model EcH$_2$O-iso provided the hydrological environment to improve confidence in the robustness of simulated hydrological

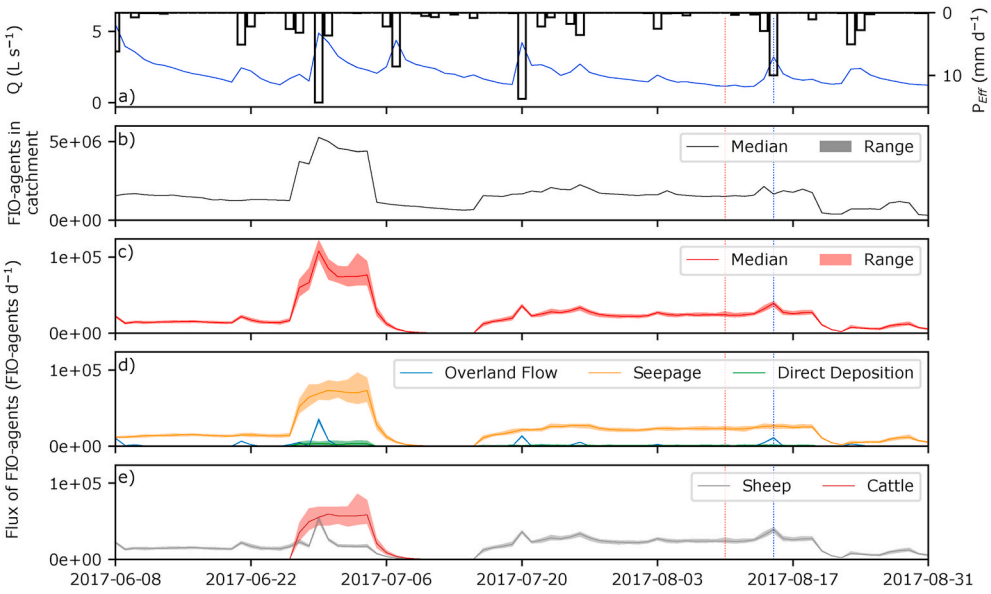

Fig. 9. Timeseries of a) Effective precipitation and discharge simulated by the "best" ensemble run of EcH_2O-iso; and b) FIO-agents stored in the catchment at the end of each timestep; c) Flux of FIO-agents exported from the catchment; d) Mechanisms by which exported FIO-agents reached the stream; e) Contributions of exported FIO-agents from sheep and cattle, based on the 30 ensemble runs of MAFIO. The red and blue dashed lines denote the example dry and wet days, respectively. All scales are linear. (For interpretation of the references to colour in this figure legend, the reader is referred to the Web version of this article.)

processes underpinning FIO simulations (c.f. Birkel and Soulsby, 2015; Neill et al., 2019). However, whilst multi-criteria calibration to discharge and isotope data allowed elements of catchment hydrological functioning to be reasonably constrained (i.e. dominance of groundwater, generation of overland flow proximal to the stream), uncertainty persisted in the exact spatial extent of overland flow paths (Fig. 7c). This can obscure whether deficiencies in FIO simulations arise from uncertainty in simulated hydrology or the need to refine process conceptualisation in MAFIO; where this may be an issue is highlighted in the discussion that follows. This also necessitates that a full quantitative uncertainty analysis be the subject of future work (c.f. Beven and Lamb, 2017), and reinforces the need for collection of diverse datasets for use in constraining highly-parametrised models (Kelleher et al., 2017; Kuppel et al., 2018b).

The consistent simulation of zero loads of *E. coli* at T8 despite non-zero loads being observed likely indicates that process conceptualisation in MAFIO itself requires refinement (Fig. 8e). This assertion arises from confidence in the lack of surface connectivity between T8 and Top Pasture (the only upstream source of livestock-derived FIOs) simulated by the "best" run of EcH_2O-iso (Fig. 5b), despite the overall uncertainty in the exact extent of overland flow paths (Fig. 7c). Specifically, the skill of this run in capturing observed isotope dynamics at T8 (Fig. 4j) indicates that no overland flow upstream of this site is plausible. Furthermore, increased tree water use in the forest separating T8 and Top Pasture (Douinot et al., 2019) combined with likely enhanced filtering of FIOs in overland flow by the forest floor (Kay et al., 2012) suggests there would be limited opportunities for surface transport of FIOs between these locations. Given that deer and hares have been observed in the forest around T8, a possible refinement to MAFIO could be inclusion of wild animals as sources of FIOs. Indeed, wildlife (including gastropods, frogs and fish as previously unrecognised sources; Frick et al., 2018) have previously been found to significantly impact microbial water quality, even in agricultural areas (Muirhead et al., 2011). An alternative refinement could be accounting for possible sources of "naturalised" FIOs that have adapted to persist and grow in the environment (e.g. Jang et al., 2017). A key issue to consider when conceptualising the former would be the increased uncertainty in loading and die-off parameters associated with FIOs from wildlife (Guber et al., 2015). Furthermore, difficulties also exist in characterising population levels and movement of wild animals in the landscape (Tetzlaff et al., 2010); however, these could likely be accommodated by representing wildlife behaviour stochastically in MAFIO. Whilst this would probably result in greater stochastic variability across ensemble simulations, it would help increase confidence that the potential impacts of wildlife as a source of FIOs are being represented.

This last point is relevant when inferring process adequacy from the large spread in non-zero loads simulated at T6 (Fig. 8c–d). As there were again no surface flow paths upstream of this site in the simulated hydrological environment (Fig. 5b), FIO-agents could only be directly deposited in the stream by livestock in Mid Pasture (R). Given the stochastic treatment of livestock movement and, consequently, direct deposition in MAFIO, it should be expected that different ensemble runs will collectively simulate a range of possible *E. coli* loads dependent on when and where livestock were simulated to directly defecate in the stream (c.f. Abdou et al., 2012). Given the plausibility of direct deposition influencing microbial water quality at T6 when livestock are present in Mid Pasture (R) due to stream accessibility (Fig. 1c), observed loads may reflect one particular realisation of how livestock entered the stream and directly deposited (c.f. Windrum et al., 2007). Consequently, that observations could fall within the spread of simulated loads (Fig. 8c–d) likely suggests that MAFIO is adequately representing the process of direct deposition. Thus, it cannot be concluded that the large spread in simulated non-zero loads is indicative of model inadequacy (c.f. Parker and Meretsky, 2004).

A more problematic feature of simulations at T6 is the consistent simulation of zero loads when livestock were absent from Mid Pasture (R) despite observed non-zero loads (Figs. 3f and 8c). This could reflect incorrect simulation of zero loads at T8, depending on the extent to which upstream locations influence microbial water quality at T6 (Neill et al., 2018; Vitro et al., 2017). Qualitative similarity between observed *E. coli* dynamics at T6 and T8 when livestock were absent from Mid Pasture (R) lends some support to this possibility (Fig. 3c–d and f). However, uncertainty in the exact spatial extent of flow paths simulated by EcH_2O-iso also means that surface connectivity between Mid Pasture (R) and the stream could have plausibly been simulated by some behavioural model runs. Such connectivity could facilitate transfer of FIOs to the stream in the absence of livestock, depending on longevity of survival (Martinez et al., 2013). Consequently, further work to reduce uncertainty in simulated flow paths is necessary to determine whether under-predictions at T6 have a hydrological or microbiological cause. A further possibility could be that a streambed reservoir of *E. coli* from livestock in Mid Pasture (R) exists that can be mobilised by streamflow (McDonald et al., 1982). However, this mechanism would be unlikely to explain under-predictions that occurred during times of recessional and

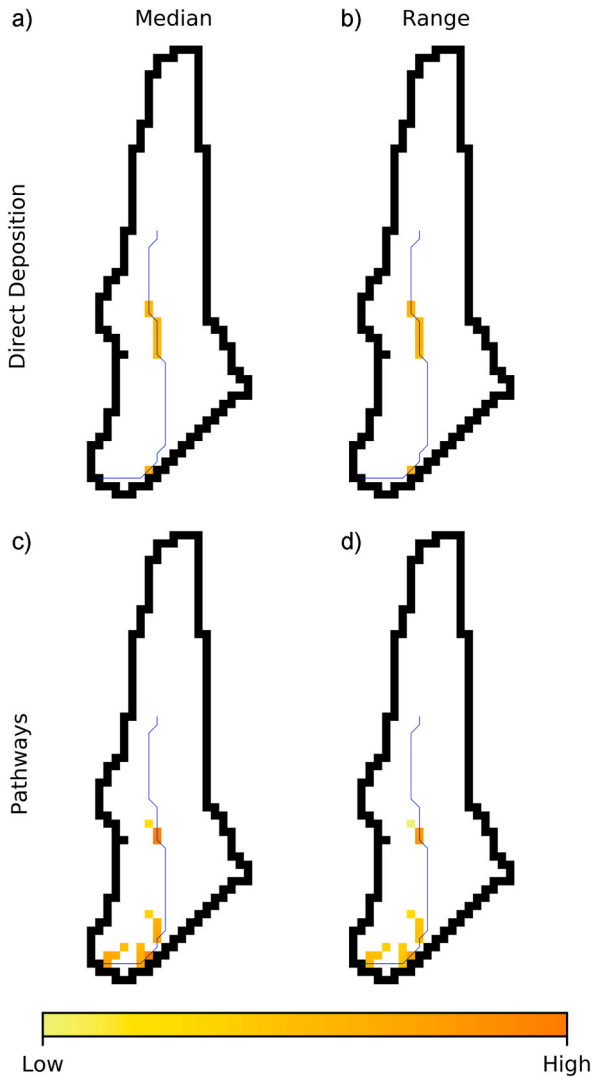

Fig. 10. For the whole microbial observation period and based on the 30 ensemble runs of MAFIO, maps showing the a) Median number and b) Range in numbers of exported FIO-agents directly deposited in the stream for each cell containing a channel, and pathways based on the c) Median number or d) Range in numbers of FIO-agents that passed through each grid cell in the course of being transported to the stream in overland flow or seepage. The scale reflects the $\log_{10}$-transformed median number/range in numbers and is common to all maps. Areas of white denote medians/ranges of 0.

base flows (Figs. 3a and 8c; Nagels et al., 2002).

Despite the tendency to over-estimate loads in absolute terms, MAFIO had most skill in capturing observed *E. coli* dynamics at the outlet (Fig. 8a–b). Furthermore, stochastic variability in simulations was reduced compared to T6 (Fig. 8a–d). Combined, these results suggest that potential process deficiencies impacting upstream sites had less influence here. This likely reflected greater opportunities for FIO-agents to reach the stream via seepage and transport in overland flow generated by areas proximal to the stream in the lower catchment (Figs. 1c, 5 and 9). The promising performance of MAFIO at the outlet suggests that it reasonably well-captures these highly-localised mechanisms of FIO transfer as dominant drivers of impaired microbial water quality at this location. This is further supported by relative confidence in the simulation of overland flow generation close to the stream and of soil saturation deficits underpinning seepage (Fig. 7a and d) by EcH_2O-iso, and would also be consistent with the likely importance of near-stream sources of FIOs in the wider Tarland Burn (Neill et al., 2018). The over-estimation of loads at the outlet, however, highlights there is scope for improving the degree to which simulations capture the detail in observations. Consequently, several avenues for model refinement are identified that may help increase correspondence between observed and simulated loads at the outlet and lead to more nuanced simulation of FIO dynamics in general.

Many parameters relating to the loading, die-off, and transport of FIOs are characterised by uncertainty (Cho et al., 2016). Therefore, in addition to a quantitative assessment of how flow path uncertainty in EcH_2O-iso affects MAFIO simulations, a sensitivity analysis and calibration of MAFIO parameters should also be conducted. This may help better-constrain parameters and improve simulations whilst enhancing understanding of how parameter uncertainty is propagated into model outputs (e.g. Beven, 2006). However, limitations in using "fit-to-data" metrics to assess ABM performance likely means that alternative automated calibration procedures will need developing (c.f. Polhill and Salt, 2017). MAFIO has also been applied at relatively coarse spatial (30×30 m) and temporal (1-day timestep) resolutions in this initial application. Whilst this spatial scale is finer than permitted by most process-based FIO models (e.g. Dorner et al., 2006; Whitehead et al., 2016), resolving non-linearities in the fate and transport of FIOs arising from the effects of small-scale heterogenity in the landscape (e.g. micro-topography influencing flow paths; Frei et al., 2010) or processes operating at sub-daily timescales (e.g. intra-storm precipitation dynamics; McKergow and Davies-Colley, 2010) may be necessary for more nuanced simulation of FIO dynamics. Finally, alternative methods of allowing MAFIO to simulate the large populations of FIOs found in catchments could be trialled. One possibility is use of "super-individuals" (Scheffer et al., 1995). Like FIO-agents, these are introduced into a simulation for every given number of real individuals. However, this number is then assigned to the super-individual as an attribute that is influenced by controlling processes, which may give a more complete simulation of dynamics that would be observed if all individuals were represented explicitly (Scheffer et al., 1995). Exploring these avenues for model refinement will be a focus of future work.

5.2. *What potential does MAFIO have for providing process-based insights into microbial water quality that are relevant for management?*

The preceding discussion highlights the status of MAFIO as a research-level model. However, application to Tulloch Burn still provided insight into how an agent-based approach has significant potential for identifying drivers of microbial water quality at scales relevant for management.

Management of microbial water quality at the farm scale is always likely to have financial implications for the farmer (Oliver et al., 2007). Consequently, information aiding spatial targeting of cost-effective and efficient mitigation measures is desirable (c.f. Oliver et al., 2018; Vinten et al., 2017). The facility to interrogate the *Domain type memory* and *Location memory* attributes of exported FIO-agents in MAFIO permits insights into the transfer mechanisms and source areas contributing FIOs to streams, which may have significant value in this respect. For the Tulloch Burn, for example, it was revealed that whilst overland flow could cause spikes in the flux of exported FIO-agents during events, its capacity to transport FIO-agents to the stream in time and space was overall limited (Figs. 9–11). Consequently, seepage from areas of degraded soil was always the dominant transfer mechanism (Fig. 9d) and exported FIO-agents were sourced from locations highly proximal to the stream under all conditions (Figs. 10–11). As the skill of MAFIO in simulating observed *E. coli* dynamics at the outlet suggests these localised mechanisms are dominant drivers of microbial water quality (Fig. 8a–b), an implication is that small-scale interventions (e.g. building bridges between fields separated by the stream or preventing livestock access to stream-proximal locations capable of generating overland flow) could result in significant improvements to microbial water quality without the need for larger-scale and more costly measures (e.g. reducing stocking densities or extensive use of buffer strips; Cuttle et al.,

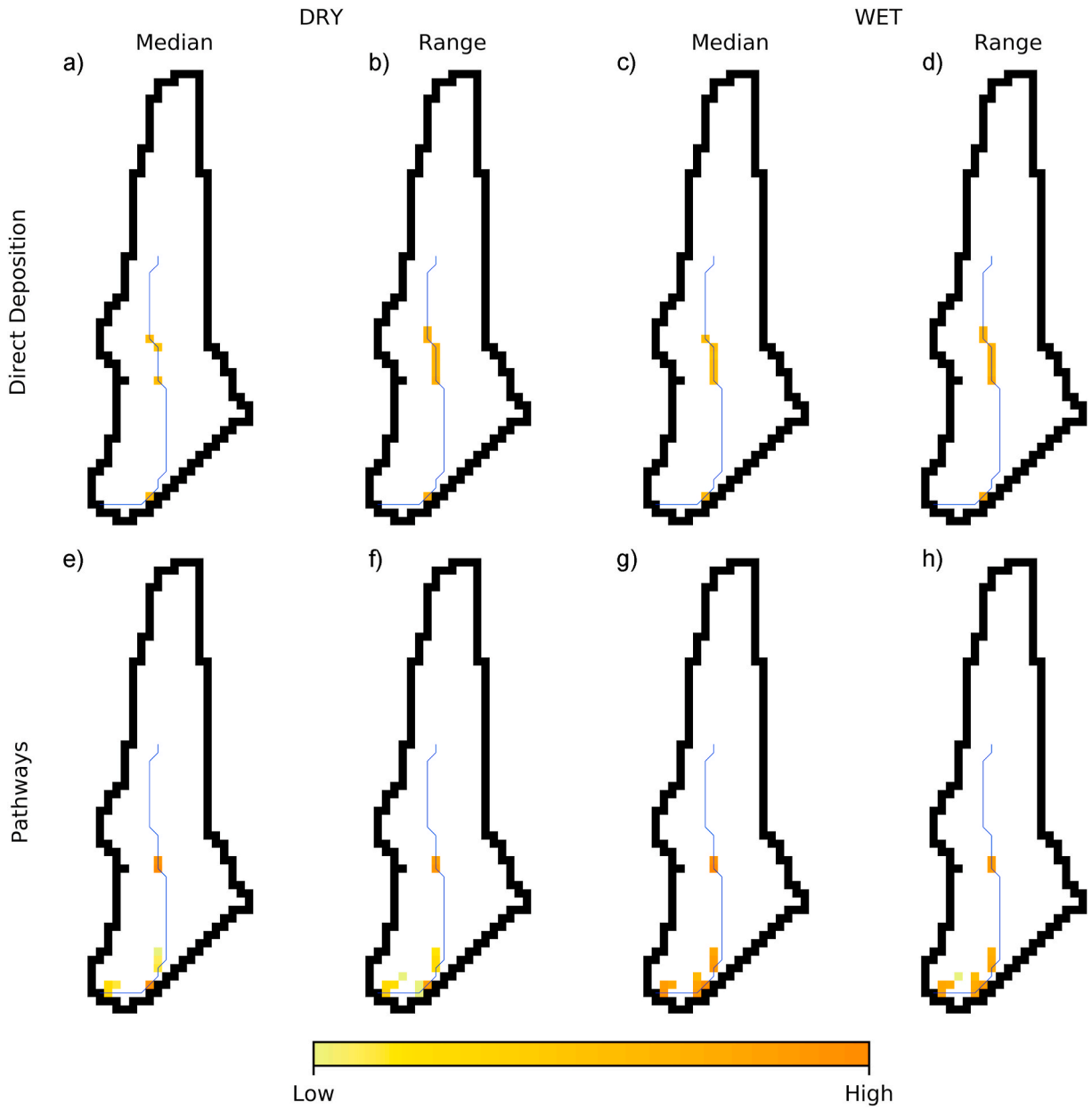

Fig. 11. For the exemplar dry day and based on the 30 ensemble runs of MAFIO, maps showing the a) Median number and b) Range in numbers of exported FIO-agents directly deposited in the stream for each cell containing a channel, and pathways based on the e) Median number or f) Range in numbers of FIO-agents that passed through each grid cell in the course of being transported to the stream in overland flow or seepage. Equivalent maps for the wet day are shown in (c–d) and (g–h), respectively. The scale reflects the $\log_{10}$-transformed median number/range in numbers and is common to all maps. Areas of white denote medians/ranges of 0.

2006).

Quantitative microbial risk assessment (QMRA) can further assist in selection of mitigation measures by providing a basis for assessing how risks presented by faecal pathogens to human health can be reduced through management (Haas et al., 2014; Strachan et al., 2005). Usually, a dose-response model estimates the likelihood of an adverse health effect occurring based on an input dosage of pathogens (Haas et al., 2014). Direct quantification of pathogens in water is not common, however, due to their lower occurrence with respect to FIOs and the costly methods necessary for their enumeration (Geldreich, 1996). Therefore, it may be necessary to estimate exposure based on the prevalence of pathogens in animals responsible for contaminating the medium humans come into contact with (c.f. Strachan et al., 2002). In this regard, MAFIO simulations attributing contributions of exported FIO-agents to different livestock types (Fig. 9e) could prove useful. Furthermore, the agent-based model structure could allow direct simulation of pathogenic organisms alongside non-pathogenic FIOs, subject to sufficient data availability to inform parameterisations or rule sets associated with pathogenic FIO-agents (c.f. Hipsey et al., 2008).

The ability to model processes stochastically in MAFIO may also be of value in a management context. In particular, this can enable greater representation of how both natural variability and uncertainty in simulated processes propagate to predictions of microbial water quality, which may be useful for decision making (c.f. Brouwer and De Blois, 2008). Indeed, application of MAFIO to the Tulloch Burn highlighted how simulated *E. coli* loads may demonstrate considerable spread due to variability and uncertainty in how livestock use the landscape and, consequently, directly defecate in streams (c.f. Oliver et al., 2010). However, full realisation of this value would be contingent on the development of appropriate calibration methods for ABMs which

quantify how parameter and structural uncertainty also propagate to model outputs, as discussed earlier.

A final important point relates to the data requirements of MAFIO and its consequent transferability. As previously highlighted, availability of diverse observations corresponding to model outputs will benefit calibration/validation of the model and its associated hydrological environment simulator (c.f. Kelleher et al., 2017; Kuppel et al., 2018b). However, where such observations exist, it is not necessary that model inputs be derived from site-specific data such as those available in this study following intensive monitoring at the Tulloch Burn. For example, nationally-available datasets combined with simple assumptions regarding grazing practices could provide the spatial arrangement of fields within a catchment along with livestock counts that vary in space and time (e.g. Oliver et al., 2010, 2018). Furthermore, use of local datasets (e.g. regarding stream fencing as in Dymond et al., 2016) alongside one-off farm surveys or farmer interviews (Oliver et al., 2007, 2009) could sufficiently characterise the spatial distributions of stream accessibility to livestock and areas of degraded soil. Other necessary catchment characteristics can be derived from widely-available data (e.g. elevation, soil types, etc.) integrated into a geographical information system. Finally, where site-specific data on FIO concentrations in faeces and soil are unavailable, estimates may be derived from literature values (e.g. Dorner et al., 2006; Hipsey et al., 2008; Whitehead et al., 2016). Consequently, it should be possible to apply MAFIO to less intensively-studied catchments. It is also important to emphasise that any hydrological model could be used to provide the hydrological environment for MAFIO as long as its consistency with catchment hydrological functioning can be robustly assessed.

6. Conclusions

This work provided a proof-of-concept application for MAFIO, an agent-based model designed to unravel the spatio-temporal dynamics of sources and transfer mechanisms contributing FIOs to streams at the sub-field scale. Performance in simulating observed *E. coli* dynamics in the Tulloch Burn catchment showed that the model has skill in capturing the transfer of FIOs from livestock to streams via the processes of direct deposition, overland flow and seepage from areas of degraded soil. This assessment was aided by EcH$_2$O-iso, the hydrological environment simulator for MAFIO, identifying generation of overland flow close to the stream and dominance of groundwater in the catchment with some confidence following multi-criteria calibration to discharge and isotope data. However, uncertainty in the exact spatial extent of overland flow paths simulated by EcH$_2$O-iso meant it was not always clear whether deficiencies in MAFIO performance reflected a hydrological or microbiological cause. This identified the need for a quantitative assessment of uncertainty propagation from EcH$_2$O-iso to MAFIO to be the subject of future work. Nonetheless, under-prediction of observed *E. coli* loads in the upper catchment implied the need to consider "naturalised" or wildlife sources of FIOs in the model, and it was further possible to identify several avenues relating to issues of scale and calibration that could be explored to improve model performance.

Despite the present status of MAFIO as a research-level model, this application revealed how the agent-based structure of the model allowed it to have significant potential for informing management. Interrogation of the attributes of FIO-agents exported from the catchment could reveal insights into source areas, transfer mechanisms and livestock contributing FIOs to the stream, providing information that could inform implementation of efficient, cost-effective mitigation measures. Furthermore, the potential to model processes stochastically in MAFIO allowed the effects of natural variability and uncertainty in processes influencing microbial water quality to be characterised, which may have value in a decision support context. Whilst this proof-of-concept study identified possible refinements that could be made to MAFIO, once addressed, it is likely that the model could have substantial value in underpinning decision support frameworks aimed at mitigating impaired microbial water quality.

Software and data availability

The source code for MAFIO as used in this work is available via the University of Aberdeen PURE repository: https://doi.org/10.20392/66f74663-ece3-4a52-8bed-f0cf52d0831a.

The source code for EcH$_2$O-iso is available at: https://bitbucket.org/sylka/ech2o_iso/src/master_2.0/.

The Tulloch Burn datasets used in this study are available from the lead author on request.

Declaration of competing interest

The authors declare that they have no known competing financial interests or personal relationships that could have appeared to influence the work reported in this paper.

CRediT authorship contribution statement

Aaron J. Neill: Conceptualization, Methodology, Software, Formal analysis, Investigation, Data curation, Writing - original draft, Writing - review & editing, Visualization. **Doerthe Tetzlaff:** Conceptualization, Methodology, Resources, Writing - original draft, Writing - review & editing, Supervision, Project administration, Funding acquisition. **Norval J.C. Strachan:** Conceptualization, Methodology, Resources, Writing - original draft, Writing - review & editing, Supervision, Funding acquisition. **Rupert L. Hough:** Conceptualization, Methodology, Resources, Writing - original draft, Writing - review & editing, Supervision, Funding acquisition. **Lisa M. Avery:** Conceptualization, Methodology, Resources, Writing - original draft, Writing - review & editing, Supervision, Investigation. **Marco P. Maneta:** Methodology, Software. **Chris Soulsby:** Conceptualization, Methodology, Resources, Writing - original draft, Writing - review & editing, Supervision, Project administration, Funding acquisition.

Acknowledgments

Funding for this work from the Scottish Government's Hydro Nation Scholars Programme is gratefully acknowledged. Many thanks to Audrey Innes, Jonathan Dick, Claire Tunaley and Bernhard Scheliga for their assistance in analysing the isotope samples. In addition, thanks to Allan Sim, Duncan White and, in particular, Claire Abel and Adam Wyness for instruction and training on microbiological sampling and analysis techniques. Simulations with EcH$_2$O-iso and MAFIO were undertaken on the Maxwell high performance computing cluster funded by the University of Aberdeen. Sylvain Kuppel and Aaron Smith are thanked for their assistance in troubleshooting occasional issues with EcH$_2$O-iso.

Appendix A. Supplementary data

Supplementary data to this article can be found online at https://doi.org/10.1016/j.jenvman.2020.110905.

References

Abdou, M., Hamill, L., Gilbert, N., 2012. Designing and building an agent-based model: 141-166. In: Heppenstall, A.J., Crooks, A.T., See, L.M., Batty, M. (Eds.), Agent-Based Models of Geographical Systems. Springer, Dordrecht, Heidelberg, London, New York.

Ala-aho, P., Tetzlaff, D., McNamara, J.P., Laudon, H., Soulsby, C., 2017. Using isotopes to constrain water flux and age estimates in snow-influenced catchments using the STARR (Spatially distributed Tracer-Aided Rainfall-Runoff) model. Hydrological Earth Systems Science 21, 5089–5110.

Bergfur, J., Demars, B.O.L., Stutter, M.I., Langan, S.J., Friberg, N., 2012. The Tarland catchment initiative and its effect on stream water quality and macroinvertebrate indices. J. Environ. Qual. 41, 314–321.

Beven, K., 2006. A manifesto for the equifinality thesis. J. Hydrol. 320, 18–36.
Beven, K., 2012. Rainfall-runoff Modelling: the Primer, second ed. John Wiley and Sons, Chichester, UK.
Beven, K., 2019. Towards a methodology for testing models as hypotheses in the inexact sciences. Proc. Roy. Soc. A 475, 20180862.
Beven, K., Lamb, R., 2017. The uncertainty cascade in model fusion. Geological Society, London, Special Publications 408, 255–266.
Bilotta, G.S., Brazier, R.E., Haygarth, P.M., 2007. The impacts of grazing animals on the quality of soils, vegetation and surface waters in intensively managed grasslands. Adv. Agron. 94, 237–280.
Birkel, C., Soulsby, C., 2015. Advancing tracer-aided rainfall-runoff modelling: a review of progress, problems and unrealised potential. Hydrol. Process. 29, 5227–5240.
Brouwer, R., De Blois, C., 2008. Integrated modelling of risk and uncertainty underlying the cost and effectiveness of water quality measures. Environ. Model. Software 23, 922–937.
Brown, D.G., Page, S., Riolo, R., Zellner, M., Rand, W., 2005. Path dependence and the validation of agent-based spatial models of land use. Int. J. Geogr. Inf. Sci. 19, 153–174.
Cho, K.H., Pachepsky, Y.A., Oliver, D.M., Muirhead, R.W., Park, Y., Quilliam, R.S., Shelton, D.R., 2016. Modelling fate and transport of fecally-derived microorganisms at the watershed scale: state of the science and future opportunities. Water Res. 100, 38–56.
Cuttle, S.P., Macleod, C.J.A., Chadwick, D.R., Scholefield, D., Haygarth, P.M., Newell-Price, P., Harris, D., Shepherd, M.A., Chambers, B.J., Humphrey, R., 2006. An Inventory of Methods to Control Diffuse Water Pollution from Agriculture (DWPA): User Manual. Accessed July 2019 from. http://randd.defra.gov.uk/Document.aspx?Document=es0203_4145_FRA.pdf.
Dee, D.P., Uppala, S.M., Simmons, A.J., Berrisford, P., Poli, P., Kobayashi, S., Andrae, U., Balmaseda, M.A., Balsamo, G., Bauer, P., Bechtold, P., Beljaars, A.C.M., van de Berg, L., Bidlot, J., Bormann, N., Delsol, C., Dragani, R., Fuentes, M., Geer, A.J., Haimberger, L., Healy, S.B., Hersbach, H., Holm, E.V., Isaksen, L., Kållberg, P., Kohler, M., Matricardi, M., McNally, A.P., Monge-Sanz, B.M., Morcrette, J.-J., Park, B.-K., Peubey, C., de Rosnay, P., Tavolato, C., Thepaut, J.-N., Vitart, F., 2011. The ERA-Interim reanalysis: configuration and performance of the data assimilation system. Q. J. R. Meteorol. Soc. 137, 553–597.
Dorner, S.M., Anderson, W.B., Slawson, R.M., Kouwen, N., Huck, P.M., 2006. Hydrologic modeling of pathogen fate and transport. Environ. Sci. Technol. 40, 4746–4753.
Douinot, A., Tetzlaff, D., Maneta, M., Kuppel, S., Schulte-Bisping, H., Soulsby, C., 2019. Ecohydrological modelling with EcH$_2$O-iso to quantify forest and grassland effects of water partitioning and flux ages. Hydrol. Process. 33, 2174–2191.
Dunn, S.M., Johnston, L., Taylor, C., Watson, H., Cook, Y., Langan, S.J., 2013. Capability and limitations of a simple grid-based model for simulating land use influences on stream nitrate concentrations. J. Hydrol. 507, 110–123.
Dymond, J.R., Serezat, D., Ausseil, A.G.E., Muirhead, R.W., 2016. Mapping of Escherichia coli sources connected to waterways in the Ruamahanga catchment, New Zealand. Environ. Sci. Technol. 50 (4), 1897–1905.
Frei, S., Lischeid, G., Fleckenstein, J.H., 2010. Effects of micro-topography on surface–subsurface exchange and runoff generation in a virtual riparian wetland – a modeling study. Adv. Water Resour. 13 (11), 1388–1401.
Frick, C., Vierheilig, J., Linke, R., Savio, D., Zornig, H., Antensteiner, R., Baumgartner, C., Bucher, C., Blaschke, A.P., Derx, J., Kirschner, A.K.T., Ryzinska-Paier, G., Mayer, R., Seidl, D., Nadiotis-Tsaka, T., Sommer, R., Farnleitner, A.H., 2018. Poikilothermic animals as a previously unrecognized source of fecal indicator bacteria in a backwater ecosystem of a large river. Appl. Environ. Microbiol. 84, e00715–e00718.
Geldreich, E.E., 1996. Pathogenic agents in freshwater resources. Hydrol. Process. 10, 315–333.
Goody, R.M., Yung, Y.L., 1995. Atmospheric Radiation: Theoretical Basis. Oxford University Press, Oxford, UK.
Greene, S., Johnes, P.J., Bloomfield, J.P., Reaney, S.M., Lawley, R., Elkhatib, Y., Freer, J., Odoni, N., Macleod, C.J.A., Percy, B., 2015. A geospatial framework to support integrated biogeochemical modelling in the United Kingdom. Environ. Model. Software 68, 219–232.
Guber, A.K., Fry, J., Ives, R.L., Rose, J.B., 2015. Escherichia coli survival in, and release from, white-tailed deer feces. Appl. Environ. Microbiol. 81, 1168–1176.
Gupta, H.V., Kling, H., Yilmaz, K.K., Martinez, G.F., 2009. Decomposition of the mean squared error and NSE performance criteria: implications for improving hydrological modelling. J. Hydrol. 377, 80–91.
Hannaford, J., Muchan, K., Lewis, M., Clemas, S., 2018. Hydrological Summary for the United Kingdom: December 2017. NERC/Centre for Ecology & Hydrology, Wallingford, UK. Accessed June 2019 from. http://nora.nerc.ac.uk/id/eprint/518984/.
Haas, C.N., Rose, J.B., Gerba, C.P., 2014. Quantitative Microbial Risk Assessment, second ed. Wiley, Hoboken, New Jersey.
Haydon, S., Deletic, A., 2006. Development of a coupled pathogen-hydrologic catchment model. J. Hydrol. 328, 467–480.
Hipsey, M.R., Antenucci, J.P., Brookes, J.D., 2008. A generic, process-based model of microbial pollution in aquatic systems. Water Resour. Res. 44, W07408.
Hrachowitz, M., Soulsby, C., Tetzlaff, D., Speed, M., 2010. Catchment transit times and landscape controls—does scale matter? Hydrol. Process. 24, 117–125.
Jang, J., Hur, H.-G., Sadowsky, M.J., Byappanahalli, M.N., Yan, T., Ishii, S., 2017. Environmental Escherichia coli: ecology and public health implications—a review. J. Appl. Microbiol. 123, 570–581.
Kay, D., Crowther, J., Kay, C., Mcdonald, A.T., Ferguson, C., Stapleton, C.M., Wyer, M.D., 2012. Effectiveness of best management practices for attenuating the transport of livestock-derived pathogens within catchments: 195-255. In: Dufour, A., Bartram, J., Bos, R., Gannon, V. (Eds.), Animal Waste, Water Quality and Human Health. IWA Publishing, London.
Kay, D., Crowther, J., Stapleton, C.M., Wyer, M.D., Fewtrell, L., Anthony, S., Bradford, M., Edwards, A., Francis, C.A., Hopkins, M., Kay, C., McDonald, A.T., Watkins, J., Wilkinson, J., 2008. Faecal indicator organism concentrations and catchment export coefficients in the UK. Water Res. 42, 2649–2661.
Kelleher, C., McGlynn, B., Wagener, T., 2017. Characterising and reducing equifinality by constraining a distributed catchment model with regional signatures., local observations and process understanding. Hydrol. Earth Syst. Sci. 21, 3325–3352.
Krause, P., Boyle, D.P., Bäse, F., 2005. Comparison of different efficiency criteria for hydrological model assessment. Adv. Geosci. 5, 89–97.
Kuppel, S., Tetzlaff, D., Maneta, M.P., Soulsby, C., 2018a. EcH2O-iso 1.0: water isotopes and age tracking in a process-based, distributed ecohydrological model. Geosci. Model Dev. (GMD) 11, 3045–3069.
Kuppel, S., Tetzlaff, D., Maneta, M.P., Soulsby, C., 2018b. What can we learn from multi-criteria calibration of a process-based ecohydrological model? Environ. Model. Software 101, 301–316.
Langan, S.J., Wade, A.J., Smart, R.P., Edwards, A.C., Soulsby, C., Billett, M.F., Jarvie, H. P., Cresser, M.S., Owen, R., Ferrier, R.C., 1997. The prediction and management of water quality in a relatively unpolluted major Scottish catchment: current issues and experimental approaches. Sci. Total Environ. 194–195, 419–435.
Legates, D.R., McCabe, G.J., 1999. Evaluating the use of "goodness-of-fit" measures in hydrologic and hydroclimatic model validation. Water Resour. Res. 35, 233–241.
Martinez, G., Pachepsky, Y.A., Shelton, D.R., Whelan, G., Zepp, R., Molina, M., Panhorst, K., 2013. Using the Q_{10} model to simulate *E. coli* survival in cowpats on grazing lands. Environ. Int. 54, 1–10.
McDonald, A., Kay, D., Jenkins, A., 1982. Generation of fecal and total coliform surges by stream flow manipulation in the absence of normal hydrometeorological stimuli. Appl. Environ. Microbiol. 44, 292–300.
McKergow, L.A., Davies-Colley, R.J., 2010. Stormflow dynamics and loads of *Escherichia coli* in a large mixed land use catchment. Hydrol. Process. 24, 276–289.
Morris, M.D., 1991. Factorial sampling plans for preliminary computational experiments. Technometrics 33, 161–174.
Moss, S., Edmonds, B., 2005. Sociology and simulation: statistical and qualitative cross-validation. Am. J. Sociol. 110, 1095–1131.
Muirhead, R.W., 2009. Soil and faecal material reservoirs of Escherichia coli in a grazed pasture. N. Z. J. Agric. Res. 52, 1–8.
Muirhead, R.W., Elliot, A.H., Monaghan, R.M., 2011. A model framework to assess the effect of dairy farms and wild fowl on microbial water quality during base-flow. Water Res. 45, 2863–2874.
Nagels, J.W., Davies-Colley, R.J., Donnison, A.M., Muirhead, R.W., 2002. Faecal contamination over flood events in a pastoral agricultural stream in New Zealand. Water Sci. Technol. 45, 45–52.
Neill, A.J., Tetzlaff, D., Strachan, N.J.C., Soulsby, C., 2019. To what extent does hydrological connectivity control dynamics of faecal indicator organisms in streams? Initial hypothesis testing using a tracer-aided model. J. Hydrol. 570, 423–435.
Neill, A.J., Tetzlaff, D., Strachan, N.J.C., Hough, R.L., Avery, L.M., Watson, H., Soulsby, C., 2018. Using spatial-stream-network models and long-term data to understand and predict dynamics of faecal contamination in a mixed land-use catchment. Sci. Total Environ. 612, 840–852.
Neill, A.J., Tetzlaff, D., Strachan, N.J.C., Hough, R.L., Avery, L.M., Kuppel, S., Maneta, M. P., Soulsby, C., 2020. An agent-based model that simulates the spatio-temporal dynamics of sources and transfer mechanisms contributing faecal indicator organisms to streams. Part 1: background and model description. J. Environ. Manag. https://doi.org/10.1016/j.jenvman.2020.110903.
O'Sullivan, D., Millington, J., Perry, G., Wainwright, J., 2012. Agent-based models – because they're worth it? In: Heppenstall, A.J., Crooks, A.T., See, L.M., Batty, M. (Eds.), Agent-Based Models of Geographical Systems. Springer, Dordrecht, Heidelberg, London, New York, pp. 109–123.
Oliver, D.M., Heathwaite, A.L., Hodgson, C.J., Chadwick, D.R., 2007. Mitigation and current management attempts to limit pathogen survival and movement within farmed grassland. Adv. Agron. 93, 95–152.
Oliver, D.M., Bartie, P.J., Heathwaite, A.L., Reaney, S.M., Parnell, J.A.Q., Quilliam, R.S., 2018. A catchment-scale model to predict spatial and temporal burden of *E. coli* on pasture from grazing livestock. Sci. Total Environ. 616–617, 678–687.
Oliver, D.M., Fish, R.D., Hodgson, C.J., Heathwaite, A.L., Chadwick, D.R., Winter, M., 2009. A cross-disciplinary toolkit to assess the risk of faecal indicator loss from grassland farm systems to surface waters. Agric. Ecosyst. Environ. 129, 401–412.
Oliver, D.M., Page, T., Hodgson, C.J., Heathwaite, A.L., Chadwick, D.R., Fish, R.D., Winter, M., 2010. Development and testing of a risk indexing framework to determine field-scale critical source areas of faecal bacteria on grassland. Environ. Model. Software 25, 503–512.
Oliver, D.M., Porter, K.D.H., Pachepsky, Y.A., Muirhead, R.W., Reaney, S.M., Coeffey, R., Kay, D., Milledge, D.G., Hong, E., Anthony, S.G., Page, T., Bloodworth, J.W., Mellander, P., Carbonneau, P., McGrane, S.J., Quilliam, R.S., 2016. Predicting microbial water quality with models: over-arching questions for managing risk in agricultural catchments. Sci. Total Environ. 544, 39–47.
Parker, D.C., Meretsky, V., 2004. Measuring pattern outcomes in an agent-based model of edge-effect externalities using spatial metrics. Agric. Ecosyst. Environ. 101, 233–250.
Parry, H.R., Bithell, M., 2012. Large scale agent-based modelling: a review and guidelines for model scaling: 271-308. In: Heppenstall, A.J., Crooks, A.T., See, L.M., Batty, M. (Eds.), Agent-Based Models of Geographical Systems. Springer, Dordrecht, Heidelberg, London, New York.

Polhill, J.G., Sutherland, L., Gotts, N.M., 2010. Using qualitative evidence to enhance and agent-based modelling system for studying land use change. J. Artif. Soc. Soc. Simulat. 13 (2), 10. http://jasss.soc.surrey.ac.uk/13/2/10.html.

Polhill, J.G., Salt, D., 2017. The importance of ontological structure: why validation by 'fit-to-data' is insufficient: 141-172. In: Edmonds, B., Meyer, R. (Eds.), Simulating Social Complexity: A Handbook, second ed. Springer, Dordrecht, Heidelberg, London, New York.

Porter, K.D.H., Reaney, S.M., Quilliam, R.S., Burgess, C., Oliver, D.M., 2017. Predicting diffuse microbial pollution risk across catchments: the performance of SCIMAP and recommendations for future development. Sci. Total Environ. 609, 456–465.

Reaney, S.M., 2008. The use of agent based modelling techniques in hydrology: determining the spatial and temporal origin of channel flow in semi-arid catchments. Earth Surf. Process. Landforms 33, 317–327.

Refsgaard, J.C., van der Sluijs, J.P., Højberg, A.L., Vanrolleghem, P.A., 2007. Uncertainty in the environmental modelling process – a framework and guidance. Environ. Model. Software 22, 1543–1556.

Rode, M., Arhonditsis, G., Balin, D., Kebede, T., Krysanova, V., van Griensven, A., van der Zee, S.E.A.T.M., 2010. New challenges in integrated water quality modelling. Hydrol. Process. 24, 3447–3461.

Schaefli, B., Gupta, H.V., 2007. Do Nash values have value? Hydrol. Process. 21, 2075–2080.

Scheffer, M., Baveco, J.M., DeAndelis, D.L., Rose, K.A., van Nes, E.H., 1995. Super-individuals a simple solution for modelling large populations on an individual basis. Ecol. Model. 80, 161–170.

Soheir, H., Farges, J.-L., Piet-Lahanier, H., 2014. Improvement of the representativity of the Morris Method for air-launch-to-orbit separation. IFAC Pro. Vol. 47 (3), 7954–7959.

Soil Survey of Scotland Staff, 2014. Digitized Soil Map of Scotland, Scale 1:25 000. James Hutton Institute.

Sprenger, M., Stumpp, C., Weiler, M., Aeschbach, W., Allen, S.T., Benettin, P., Dubbert, M., Hartmann, A., Hrachowitz, M., Kirchner, J.W., McDonnell, J.J., Orlowski, N., Penna, D., Pfahl, S., Rinderer, M., Rodriguez, N., Schmidt, M., Werner, C., 2019. The demographics of water: a review of water ages in the critical zone. Rev. Geophys. 57, 800–834.

Strachan, N.J.C., Dunn, G.M., Ogden, I.D., 2002. Quantitative risk assessment of human infection from *Escherichia coli* O157 associated with recreational use of animal pasture. Int. J. Food Microbiol. 75, 39–51.

Strachan, N.J.C., Doyle, M.P., Kasuga, F., Rotariu, O., Ogden, I.D., 2005. Dose response modelling of *Escherichia coli* O157 incorporating data from foodborne and environmental outbreaks. Int. J. Food Microbiol. 103, 35–47.

Tetzlaff, D., Soulsby, C., Birkel, C., 2010. Hydrological connectivity and microbiological fluxes in montane catchments: the role of seasonality and climatic variability. Hydrol. Process. 24, 1231–1235.

Vaché, K.B., McDonnell, J.J., 2006. A process-based rejectionist framework for evaluating catchment runoff model structure. Water Resour. Res. 42, W02409.

Vinten, A., Sample, J., Ibiyemi, A., Abdul-Salam, Y., Stutter, M., 2017. A tool for cost-effectiveness analysis of field scale sediment-bound phosphorus mitigation measures and application to analysis of spatial and temporal targeting in the Lunan Water catchment, Scotland. Sci. Total Environ. 586, 631–641.

Vitro, K.A., BenDor, T.K., Jordanova, T.V., Miles, B., 2017. A geospatial analysis of land use and stormwater management on fecal coliform contamination in North Carolina streams. Sci. Total Environ. 603–604, 709–727.

Wellen, C., Kamran-Disfani, A.R., Arhonditsis, G.B., 2015. Evaluation of the current state of distributed watershed nutrient water quality modeling. Environ. Sci. Technol. 49, 3278–3290.

Whitehead, P.G., Leckie, H., Rankinen, K., Butterfield, D., Futter, M.N., Bussi, G., 2016. An INCA model for pathogens in rivers and catchments: model structure, sensitivity analysis and application to the River Thames catchment, UK. Sci. Total Environ. 572, 1601–1610.

Willmott, C.J., Matsuura, K., 2005. Advantages of the mean absolute error (MAE) over the root mean square error (RMSE) in assessing average model performance. Clim. Res. 30, 79–82.

Windrum, P., Fagiolo, G., Moneta, A., 2007. Empirical validation of agent-based models: alternatives and perspectives. J. Artif. Soc. Soc. Simulat. 10 (2), 8. http://jasss.soc.surrey.ac.uk/10/2/8.html.